

APPLICATION OF THE HYDRAULIC ANALOGY TO STUDY THE PERFORMANCE
OF TWO AIRFOILS IN COMPRESSIBLE FLOW.

REF ID: A60000

Crossland

A THESIS

Presented to

The Faculty of the Division of Graduate Studies

Georgia Institute of Technology

In Partial Fulfillment

of the Requirements for the Degree

Master of Science in Aeronautical Engineering

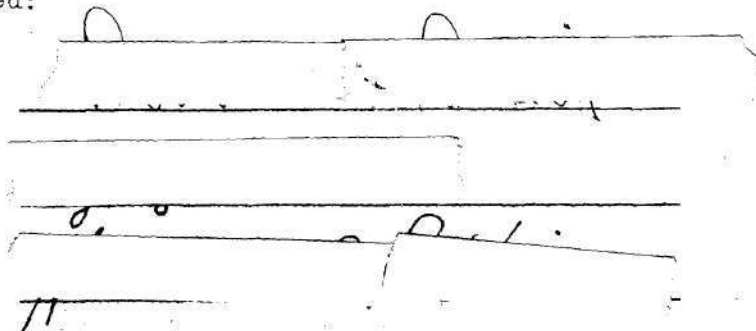
by

Eric John Catchpole

October 1949

APPLICATION OF THE HYDRAULIC ANALOGY TO STUDY THE PERFORMANCE
OF TWO AIRFOILS IN COMPRESSIBLE FLOW.

Approved:

A handwritten signature, possibly reading "D. L. ...", is written over several horizontal lines.

Date Approved by Chairman

October 28, 1949

ACKNOWLEDGEMENTS

The author wishes to express his thanks to Mr. H.W.S. LaVier for his suggestion of the topic of this thesis and for his valuable help in its execution. He also wishes to thank the shop personnel concerned for constructing the models, and Mr. Day Wood for his wholehearted assistance in the photographic work.

The helpful criticisms and suggestions of the reading committee and of the remainder of the staff of the Daniel Guggenheim School of Aeronautics were much appreciated. The author is also indebted to Dr. J.E. Rhodes, of the School of Physics, for his suggestion of the method described in Appendix III.

TABLE OF CONTENTS

	PAGE
Approval Sheet.....	ii
Acknowledgements.....	iii
List of Tables.....	v
List of Figures.....	vi
Summary.....	1
Introduction.....	2
List of Symbols.....	5
Theory.....	7
Equipment.....	12
Procedure.....	17
Tests Conducted.....	17
Comparison and Discussion.....	18
Conclusions.....	24
Recommendations.....	25
Bibliography.....	27
APPENDIX I.....	31
APPENDIX II.....	35
APPENDIX III.....	39

LIST OF TABLES

TABLE NO.	TITLE	PAGE
I	Sample Calculation of Pressure Coefficients from Experimental Data.....	32
II	Experimental Values of Lift, Drag and Moment Coefficients for G.U.3. Airfoil..	33
III	Experimental Values of Lift, Drag and Moment Coefficients for G.U.4. Airfoil..	34

LIST OF FIGURES

FIGURE NO.	TITLE	PAGE
1	General View of Water Channel.....	40
2	Carriage Drive Mechanism.....	41
3	G.U.3. Airfoil Model.....	42
4	G.U.4. Airfoil Model.....	43
5	Flow About G.U.3. Airfoil.....	44
6	Flow About G.U.4. Airfoil.....	45
7	Pressure Distribution on G.U.3. Airfoil at $M=1.85$, $\alpha = -2^\circ$	46
8	Pressure Distribution on G.U.4 Airfoil at $M=2.13$, $\alpha = 0^\circ$	47
9	Lift and Drag Curves for G.U.3. Airfoil at $M=1.85$	48
10	Lift and Drag Curves for G.U.3. Airfoil at $M=2.13$	49
11	Moment Curves for G.U.3. Airfoil at $M=1.85$	50
12	Moment Curves for G.U.3. Airfoil at $M=2.13$	51
13	Lift and Drag Curves for G.U.4. Airfoil at $M=1.85$	52

LIST OF FIGURES (Cont.)

FIGURE NO.	TITLE	PAGE
14	Lift and Drag Curves for G.U.4. Airfoil at $M = 2.13$	53
15	Moment Curves for G.U.4. Airfoil at $M = 1.85$	54
16	Moment Curves for G.U.4. Airfoil at $M = 2.13$	55
17	View of Model with Probes in Position.....	56
18	Pressure Distribution on G.U.3. Airfoil at $M = 2.13$, $\alpha = -2^\circ$: Probe Method.....	57
19	Pressure Distribution on G.U.3. Airfoil at $M = 2.13$, $\alpha = 0^\circ$: Probe Method.....	58
20	Pressure Distribution on G.U.3. Airfoil at $M = 2.13$, $\alpha = +6^\circ$: Probe Method.....	59
21	Pressure Distribution on G.U.4. Airfoil at $M = 1.85$, $\alpha = -2^\circ$: Probe Method.....	60
22	Pressure Distribution on G.U.4. Airfoil at $M = 1.85$, $\alpha = 0^\circ$: Probe Method.....	61
23	Pressure Distribution on G.U.4. Airfoil at $M = 1.85$, $\alpha = +6^\circ$: Probe Method.....	62

APPLICATION OF THE HYDRAULIC ANALOGY TO STUDY THE PERFORMANCE
OF TWO AIRFOILS IN COMPRESSIBLE FLOW.

SUMMARY

Two airfoil profiles were tested in the Georgia Institute of Technology water channel at two speeds and a range of angles of attack. By two different techniques, photographs were taken of the flow about the models and from these the water depth distribution along the airfoil profile was obtained. By application of the hydraulic analogy, the pressure distributions on the airfoils in two-dimensional supersonic gas flow were determined. These distributions, and the values of lift, drag and moment coefficients obtained from them by integration, were compared with theoretical and wind tunnel results for the same profiles in air.

INTRODUCTION

The mathematical basis for the analogy between flow of water with a free surface and two dimensional compressible gas flow was first presented by Riabouchinsky¹, and the problem has since been further investigated both fundamentally and in application.

Ernst Preiswerk² gave a conclusive proof that the methods of gas dynamics can be applied to water flow with a free surface, and the work of Binnie and Hooker in England³, and of investigators with the National Advisory Committee for Aeronautics⁴ and North American Aviation Incorporated⁵, extended and applied the theory.

Work with the analogy at the Daniel Guggenheim School of Aeronautics of the Georgia Institute of Technology was commenced by John

¹
D. Riabouchinsky, *Mecanique des fluides*. Comptes Rendus, t. 195, 1932, pp. 998-999

²
Ernst Preiswerk, "Application of the Methods of Gas Dynamics to Water Flows with Free Surface".
Part 1. "Flows with No Energy Dissipation". NACA TM No. 934, 1940
Part 2. "Flows with Momentum Discontinuities." NACA TM, No. 935, 1940

³
A. M. Binnie, and S. G. Hooker, "The Flow Under Gravity of an Incompressible and Inviscid Fluid Through a Constriction in a Horizontal Channel", Proceedings of the Royal Society. Vol. 159 (London, England) 1937. pp. 592-608

⁴
James Orlin, Norman J. Linder, and Jack G. Bitterly, "Application of the Analogy Between Water Flow with a Free Surface and Two-Dimensional Compressible Gas Flow". NACA TM, No. 1185, 1947.

⁵
J. R. Bruman, "Application of the Water Channel-Compressible Gas Analogy". North American Aviation Incorporated, Engineering Report NA-47-87, 1947.

Hatch in 1948⁶. He constructed a water channel for the purpose of making investigations relative to high speed aerodynamics, and carried out some preliminary tests with the equipment which again showed the considerable possibilities pointed out in the previous work.

Here are some of these possibilities:

(1) Visual observation may be made of flow patterns at subsonic and supersonic speeds, for the purposes of research or instruction. Features of the flow such as shock wave formation, vortices and turbulence may be observed and photographed.

(2) High supersonic Mach numbers may be obtained with model speeds of only a few feet per second.

(3) Any given Mach number may be achieved by a simple speed setting, whereas in a high speed wind tunnel it is generally necessary to change the nozzle for each Mach number. Thus with the water channel accelerated air flows may be easily simulated.

(4) Observations in the transonic region (i.e. at Mach Numbers close to unity) are possible since choking is apparently not a problem. The present investigation is most directly concerned with the last of these fields. In order that transonic observations in the water channel may be of use, it is first necessary to establish the reliability of the results in the supersonic and subsonic ranges, particular attention

John E. Hatch, "The Application of the Hydraulic Analogies to Problems of Two-Dimensional Compressible Gas Flow". Unpublished Master's thesis, Georgia Institute of Technology, Atlanta, 1949.

being paid to methods of measurement, accuracy of results, and application to air flow. In partial fulfillment of these requirements, two airfoils were tested in the Georgia Tech channel at two supersonic Mach numbers over a range of angles of attack, and comparisons made with experimental and theoretical results.

LIST OF SYMBOLS

- a - Speed of sound in gas
 C_D - Section drag coefficient
 C_L - Section lift coefficient
 C_m - Section moment coefficient, referred to leading edge
 C_p - Local pressure coefficient
 c_p - Specific heat of gas at constant pressure
 c_v - Specific heat of gas at constant volume
 γ - Adiabatic gas constant, ratio of c_p to c_v
 d - Water depth
 g - Acceleration due to gravity
 h - Enthalpy
 M - Mach number
 p - Pressure of gas
 ρ - Density of gas
 T - Absolute temperature of gas
 V - Velocity of flow
 ϕ - Velocity potential in two-dimensional flow
 α - Angle of attack
 x, y - Rectangular coordinates in the flow plane
 u, v - Components of flow velocity in x and y directions, respectively

Subscripts

No. Subscript	-	Any value of variable
l	-	Local value of variable
o	-	Value at stagnation
s	-	Value in undisturbed stream
max	-	Maximum value of variable
x	-	Partial derivative with respect to x

e.g. $\phi_x \equiv \frac{\partial \phi}{\partial x}$, $\phi_{xx} \equiv \frac{\partial^2 \phi}{\partial x^2}$

Partial derivative with respect to y

THEORY

The theory of the analogy between water flow with a free surface and two-dimensional compressible gas flow is given by Preiswerk⁹. A condensation of it is given below.

The following assumptions are made:

- (1) That the flow of the water is frictionless, so that conversion of energy into heat or internal energy is excluded.
- (2) That the vertical acceleration of the water is negligible compared with the acceleration due to gravity.
- (3) That the flow is irrotational.

The energy equations for water and for air are first considered.

For water this equation gives

$$v^2 = 2g(d_0 - d)$$

$$v_{\max} = \sqrt{2gd_0}$$

and for gas

$$v^2 = 2gc_p(T_0 - T)$$

$$v_{\max} = \sqrt{2gc_pT_0}$$

Hence $\frac{v}{v_{\max}}$ for water becomes equal to $\frac{v}{v_{\max}}$ for air if

$$\frac{d_0 - d}{d_0} = \frac{T_0 - T}{T_0}$$

that is, if

$$\frac{d}{d_0} = \frac{T}{T_0} \quad (1)$$

⁹Preiswerk. op. cit.

Thus if velocity is considered, there is an analogy between the two flows if the water depth ratio $\frac{d}{d_0}$ is compared with the gas temperature ratio $\frac{T}{T_0}$. The equations of continuity are now compared. For water this equation is

$$\frac{\partial(ud)}{\partial x} + \frac{\partial(vd)}{\partial y} = 0$$

and for two-dimensional gas flow

$$\frac{\partial(u\rho)}{\partial x} + \frac{\partial(v\rho)}{\partial y} = 0$$

Clearly the water depth d may be considered for these equations to be analogous to the gas density ρ , and hence a further condition for the analogy is

$$\frac{d}{d_0} = \frac{\rho}{\rho_0} \quad (2)$$

Comparing equations (1) and (2), it is seen that the analogy can only strictly hold if the gas is of such a nature that

$$\frac{T}{T_0} = \frac{\rho}{\rho_0} \quad (3)$$

Now the temperature and pressure of the gas must also obey the adiabatic relation

$$\left(\frac{T}{T_0}\right)^{\frac{1}{\gamma-1}} = \frac{\rho}{\rho_0} \quad (4)$$

Equations (3) and (4) can only be simultaneously satisfied if

$$\frac{1}{\gamma-1} = 1$$

that is, if

$$\gamma = 2$$

Thus the flow of water is comparable with the flow of a gas having $\gamma=2$. For air $\gamma=1.4$, but there are many quantities which do not depend strongly on the value of γ , so that the analogy has significance even for this. In particular, the supersonic pressure coefficient will be shown later in this thesis to be little affected by the value of γ if the flow deflection angle is small.

From the adiabatic relation,

$$\frac{p}{p_0} = \left(\frac{\rho}{\rho_0}\right)^\gamma = \left(\frac{\rho}{\rho_0}\right)^2$$

and therefore

$$\frac{p}{p_0} = \left(\frac{d}{d_0}\right)^2 \quad (5)$$

The velocity potential for water is given by the equation:

$$\phi_{xx} \left(1 - \frac{\phi_x^2}{g d}\right) + \phi_{yy} \left(1 - \frac{\phi_y^2}{g d}\right) - 2\phi_{xy} \frac{\phi_x \phi_y}{g d} = 0 \quad (6)$$

and the corresponding equation for a gas is

$$\phi_{xx} \left(1 - \frac{\phi_x^2}{a^2}\right) + \phi_{yy} \left(1 - \frac{\phi_y^2}{a^2}\right) - 2\phi_{xy} \frac{\phi_x \phi_y}{a^2} = 0 \quad (7)$$

The two equations (6) and (7) become identical if

$$\frac{gd}{2gd_0} = \frac{a^2}{2gh_0}$$

Thus \sqrt{gd} , which is the basic wave velocity in shallow water, corresponds to the velocity of sound a in the gas flow.

In water flowing at speeds above \sqrt{gd} , the velocity of the flow may strongly decrease for short distances and the depth may increase. An unsteady motion of this type is called a hydraulic jump, and corresponds to a shock wave in a gas.

The analogy is summarized in the following table of corresponding quantities and characteristics.

Two-Dimensional Compressible Gas Flow. $\gamma = 2$		Analogous Liquid Flow.	
Temperature ratio,	$\frac{T}{T_0}$	Water - depth ratio,	$\frac{d}{d_0}$
Density ratio,	$\frac{\rho}{\rho_0}$	Water- depth ratio,	$\frac{d}{d_0}$
Pressure ratio,	$\frac{p}{p_0}$	Square of water-depth ratio,	$\left(\frac{d}{d_0}\right)^2$
Velocity of sound,	$a = \sqrt{\frac{\gamma p}{\rho}}$	Wave velocity,	\sqrt{gd}
Mach number,	$\frac{V}{a}$	Mach number,	$\frac{V}{\sqrt{gd}}$
Shock wave		Hydraulic jump	

In the present investigation, the analogy is applied as follows:

The Mach number of the free stream may be calculated as

$$M_s = \frac{V_s}{\sqrt{g d_s}} \quad (8)$$

The pressure coefficient at any point on an airfoil is defined as

$$C_p = \frac{p_i - p_s}{\frac{1}{2} \rho_s V_s^2}$$

Now

$$\begin{aligned} \frac{1}{2} \rho_s V_s^2 &= \frac{1}{2} \rho_s a_s^2 M_s^2 \\ &= \frac{1}{2} \rho_s \left(\frac{\gamma p_s}{\rho_s} \right) M_s^2 \\ &= \frac{\gamma}{2} p_s M_s^2 \end{aligned}$$

Therefore

$$C_p = \frac{2}{\gamma M_s^2} \left[\frac{p_i}{p_s} - 1 \right]$$

Now using equation (5)

$$\begin{aligned} \frac{p_i}{p_s} &= \frac{p_i}{p_o} \cdot \frac{p_o}{p_s} = \left(\frac{d_1}{d_o} \right)^2 \left(\frac{d_o}{d_s} \right)^2 \\ &= \left(\frac{d_1}{d_s} \right)^2 \end{aligned}$$

Therefore, with $\gamma = 2$, the analogy gives the pressure coefficient as

$$C_p = \frac{1}{M_s^2} \left[\left(\frac{d_1}{d_s} \right)^2 - 1 \right] \quad (9)$$

EQUIPMENT

Two types of water channel are suitable for application of the hydraulic analogy, viz:

(1) One in which the model is stationary while water flows past it.

(2) One in which the model moves through static water.

The Georgia Tech channel is of type (2). It has the advantages over type (1) of being simpler and therefore less expensive, of enabling easy acceleration of the flow, and of having no error due to boundary effect on the bottom and sides of the channel. However, the motion of the model makes it more difficult to measure the water depth about the model, a very important factor in the quantitative use of the analogy.

A general view of the channel is shown in Figure 1. The framework is of structural steel bolted together, and supports a channel four feet wide and twenty feet long. The bottom of the channel is of quarter-inch plate glass in two five foot sections and one ten foot section, this last being located at the "test" end of the channel. The glass is supported by transverse steel members at thirty inch intervals, and a screw jack is fitted to the foot of each support leg. In this manner the model is enabled to slide over a smooth transparent surface leveled to within .01 inch throughout its length. Leveling was carried out by measuring the depth at various points

with the aid of a large spherometer; this instrument also enabled the water depth in the test section to be measured before each test to within .001 inch.

A drain is provided at one end of the channel.

The model carriage is of welded steel tubing, and has eight rubber wheels; four with horizontal axes which transfer the weight of the carriage to the channel rails and four with vertical axes which prevent sidewise movement of the carriage relative to the rails. Safety stops are provided at each end of the carriage track to prevent the carriage and model from over-running. The model is supported ahead of the carriage frame, and most of its weight is carried by the channel bottom.

The carriage is driven by a one-quarter horse-power, single phase, alternating current electric motor, through a continuous steel cable. A reversing mechanism and a "Speed-Ranger" device are installed. This system is most convenient for steady low speeds. For high speed runs, and for accelerating runs, an alternate power unit is found more suitable. This consists of a 19.5 amp, 24 volt direct current series wound motor, which drives the cable through a set of reduction gears.

In this way steady speeds of from 0.5 to 5.5 feet per second may easily be achieved. A photograph of the drive mechanisms is shown in Figure 2.

The carriage also carries a steel cam on one side which trips a microswitch on the track, thus automatically operating an electric timer for determination of the model speed.

An observation platform, located at the channel test section, supports a control panel for the timer and all necessary switches. The platform also carries mounts for the cameras used to photograph the flow about the models.

Two types of photographs are of importance in the analogy:

(1) Those from vertically above the model, showing wave patterns about the model.

(2) Those from a side position, showing the water line on the model, and thus giving the water depth distribution about the model.

The lighting and camera arrangements for type (1) has been described by Hatch¹⁰; these photographs were not taken in the present work. Photographs of type (2) were taken with a "Speed Graphic" camera mounted on the observation platform approximately 15 inches above the water line and 26 inches from the model test position. This placing gave an uninterrupted view of the water line on the model, unaffected by surrounding waves. The shutter was tripped by a solenoid operated through a microswitch in a similar manner to the timer.

Two lighting arrangements were tested for these pictures:

(1) A "Microflash" gas discharge lamp, giving a brilliant flash with a duration of two microseconds. This lamp was mounted about 20 inches vertically above the camera, and was also tripped by a micro-

¹⁰

Hatch, op. cit., pp 15-16

switch, operating a fraction of a second after the camera shutter was opened. An aperture of $f\ 5.6$ was found necessary.

(2) Two photoflood lamps, one mounted above and ahead of the test position of the model, and the other to the side of this position, so as to avoid direct reflections from the model. An aperture of $f8$ at one four-hundredth of a second was used with this arrangement.

The airfoil sections tested were chosen because of the availability of supersonic wind tunnel test results¹¹ for them. They were:

(1) Guidonia G.U.3 airfoil section, which is plane on one side and circular on the other, and is 8.8% thick.

(2) Guidonia G.U.4 airfoil section, which is triangular, and is 6.1% thick.

The models are shown in Figures 3 and 4. They were of machined hard brass with a lacquered surface, and each had a 12 inch chord. A horizontal reference line was scribed on each model from leading edge to trailing edge, 0.75 inches above the channel bottom, and vertical reference lines were scribed at one-tenth intervals of the chord. These scribed lines were used in reading the water depth about the models from the photographs.

The angle of attack of the model was determined by positioning the leading and trailing edges in relation to the channel sides

11

Antonio Ferri, "Experimental Results with Airfoils Tested in the High-Speed Tunnel at Guidonia". NACA TM No. 946, 1940

by means of a steel rule.

PROCEDURE:

Before each test run, the static water depth at the channel test section was measured and the timer reading required to obtain the desired Mach number was then calculated. With the model in place, the carriage speed was adjusted to give each desired timer reading, and a photograph was taken from the side position. The equipment used for the tests is described in the previous section.

TESTS CONDUCTED:

A static water depth of 0.22 to 0.24 inches was used. The airfoils were tested under the following conditions:

G.U.3. Airfoil.

M = 1.85, $\alpha = -2, 0, 2, 6, 10, 16$ degrees

M = 2.13 $\alpha = -2, 0, 2, 6, 10, 16$ degrees

G.U.4. Airfoil.

M = 1.85 $\alpha = 0, 2, 10$ degrees.

M = 2.13 $\alpha = 0, 2, 10$ degrees.

Each of the above test conditions was used twice to enable photographs of the upper and lower surfaces to be taken.

COMPARISON AND DISCUSSION

Since the data for the two airfoils were taken by different photographic methods, these will be discussed separately:

G.U.3. Airfoil

The G.U.3. Airfoil was photographed with the "Microflash" arrangement described in the section on equipment, and typical photographs of the upper and lower surfaces of the airfoil are shown in Figures 5(a) and 5(b) respectively. Allowance was made for the meniscus by measuring on the photograph to the bottom of the bright water line band and taking this as the true water level. A sample calculation for the pressure coefficient appears in Table I of Appendix I, and a plot of pressure coefficient against station along the chord is shown in Figure 7, with comparison curves from Ferri's wind tunnel tests at Guidonia¹² and from calculations using Busemann's parabolic formula¹³ with $\gamma = 1.4$ and $\gamma = 2$.

Values of lift, drag and moment coefficients determined from the pressure measurements are shown in Table II, and these are plotted in Figures 9, 10, 11, and 12. The plots also show comparison curves from Ferri's wind tunnel balance tests and from his calculations based on the "exact" theory.

¹²

Ferri, op. cit.

¹³

E. Arthur Bonney. "Aerodynamic Characteristics of Rectangular Wings at Supersonic Speeds". Journal of the Aeronautical Sciences. Vol. 14: 1947 pp.110-116.

The plot of Figure 7 will be discussed as being typical of the pressure coefficient curves obtained for this airfoil. It is seen from this figure that the pressure coefficient obtained by application of the analogy follows the same general trend over the airfoil surface as that indicated by supersonic theory and by wind tunnel tests, and also is of the same order of magnitude. There are some marked differences, however:

(1) The upper surface coefficient shows a sharp rise from a small positive value at the leading edge to a sharp peak of high positive value (as compared to the theoretical or wind tunnel curve) and thence at about 0.25 chord diminishes to a value close to that of the comparison curves. This peak corresponds to the hydraulic jump in water, and its width and height is mainly attributable to the lack of validity of assumption (2) of the theory; that is, for this condition the vertical acceleration of the water is not small compared to that due to gravity.

(2) The upper surface coefficient has also a considerably more positive value close to the trailing edge than does the theoretical coefficient. This corresponds more closely to the wind tunnel result, and is mainly attributable to a separation of the flow in this neighborhood.

(3) The lower surface coefficients indicate that the meniscus allowance may, if incorrect, move the whole curve by a noticeable amount.

The other contributory factor to effects (1) and (2) is the change in the pressure coefficient caused by the difference between

$\gamma=1.4$ for air and $\gamma=2$ for the hydraulic analogy, though this is shown by the theoretical curves to be of fairly small magnitude for most of the chord.

The plots of lift, drag, and moment coefficients in Figures 9, 10, 11, and 12 also show the correct trends and fair quantitative agreement with the wind tunnel and theoretical results. Since the curve of C_L against α in Figure 10 shows consistently low values of C_L , while the curve of C_L against C_m in Figure 12 shows good agreement with the values used for comparison, a consistent error in angle of attack is suggested. Later work has shown that this error probably occurred. The curves of Figure 9 show fairly close agreement with the comparisons, but at small angles of attack, as would probably be used in supersonic flight, the percentage error is considerable. At $\alpha = +2^\circ$, for example, the error in C_L is 200% if the wind tunnel curve is taken as correct.

In all cases the lift and drag coefficients approach the wind tunnel results more closely than they do the theoretical results. This arises partly from the closer agreement of the pressure plots at the trailing edge, but may also be partly coincidental, arising, for instance, from the magnitude of the leading edge pressure peak; both of these effects tend to reduce the lift coefficients.

G.U.4 Airfoil

The G.U.4 Airfoil was photographed by using photoflood lighting, as described in the equipment section, and typical photographs obtained by this method are shown in Figure 6. In this case, allowance was made for the meniscus by measuring its height from a photograph of the static model and subtracting this constant amount from the water

depth readings. The calculation of the pressure coefficient was identical to that for the G.U.3 airfoil. One plot of pressure coefficient against station along the chord is shown in Figure 8, and the values of lift, drag and moment coefficients obtained from the pressure plots are shown in Table III and in Figures 13, 14, 15, and 16. Comparison curves appear on these figures as for the G.U.3 airfoil, with the exception that a wind tunnel pressure plot is not available for this airfoil.

Similar observations to those made on the G.U.3 airfoil, as regards the leading edge pressure peak and the trend of the pressure coefficient at the trailing edge, are applicable here. Due to the smaller flow deflection angles, however, the leading edge pressure peak is less marked, and the effect of the γ change on C_p is smaller, having a maximum value of only 6%. In addition, it is worthy of note that the sudden expansion occurring in theory is reproduced in the water channel by a short but finite level drop as seen in the photograph of Figure 6(a) and reproduced in the pressure plot of Figure 8.

While the photographic method used for this airfoil allowed a smaller camera aperture and hence greater depth of focus (important at large angles of attack), the meniscus was not visible in these photographs for more than a small part of the model chord, and the use of the static meniscus height thus necessitated is rather unreliable. The meniscus height is considerably affected by the water and model surface conditions and by vertical motion of the water relative to the model. This variation is shown up by the rear half of the pressure plot of Figure 8 and by the inconsistencies of the force and moment

coefficients of Figures 13, 14, 15, and 16.

General Discussion.

The results obtained in the tests, while showing fair general qualitative and quantitative agreement with the experimental and theoretical values used for comparison, show the desirability of improvement in the measuring techniques. The form of equation (9) of the theory section,

$$C_p = \frac{1}{M_s^2} \left[\left(\frac{d_1}{d_s} \right)^2 - 1 \right]$$

itself is one which tends to give large percentage errors in C_p unless M_s , d_1 , and d_s are measured with considerable precision.

For example, if the representative case is taken for which correct values are $M_s = 2.0$, and $\frac{d_1}{d_s} = 2.0$, then the correct value of C_p is 0.75. If, however, (as was possible with the methods of measurement used in the present work) the measured values were $M_s = 2.04$, and $\frac{d_1}{d_s} = \frac{0.9\%}{1.02} \times 2.0 = 1.88$, then the measured value of C_p would be 0.61, representing a 19% error. Reduction of all component errors to 1% would for this condition cause a maximum error in C_p of 7.2%, which would represent a far more useful accuracy.

In view of the precision of measurement required, further work on the methods of measurement is desirable, particularly in the case of the local depth. One approach is to improve the photographic techniques by illumination giving a clear view of the meniscus along the length of the model. A second, and probably better, method is to use probes to determine the water depth just outside the meniscus; the improved results obtained by using this method are shown in Appendix II.

Three further points are of note when quantitative agreement is desired with wind tunnel and theoretical results for air:

(1) The leading edge pressure peak appearing on the plots is of considerable magnitude, but is smaller for smaller flow deflections. Thus for the thin airfoils likely to be used in supersonic flight, the peak would not be too marked. The widths of the peak and of the expansion drop, since their absolute values are independent of model size, could be reduced in relation to the chord by increasing the chord, and such an increase is very desirable.

(2) The effect of the change of γ from 1.4 to 2.0 is to give considerable percentage errors in, for example, the lift coefficient, at small angles of attack, even though the absolute error is not large. In the particular case of the G.U.4 airfoil at $M = 2.13$ and $\alpha = 0^\circ$, calculations from Busemann's formula give the error as about 30%. At $\alpha = 10^\circ$, however, the error is reduced to 2%.

(3) The hydraulic analogy enables only normal pressure to be considered in the determination of lift and drag coefficients, whereas the wind tunnel data for these coefficients is usually obtained with a balance, and thus includes shear effects.

CONCLUSIONS

By application of the hydraulic analogy an investigation has been carried out on the performance of two airfoils at supersonic speeds, and the results obtained have been compared with theoretical and wind tunnel results.

Good qualitative agreement with the values used for comparison has been found, except close to the airfoil leading edge or to any sharp change of curvature; but the accuracy of the experimental methods used gives only fair quantitative agreement. The values obtained are of the right order, however.

Thus the water channel has been shown to be a useful piece of equipment for two-dimensional supersonic flow investigations, particularly in regard to the qualitative work. The effect of the γ change from that for air to that for the analogy causes difficulty in quantitative agreement, particularly at small angles of attack.

After further investigations at subsonic speeds and low supersonic speeds, the water channel should present a cheap and useful means of investigating transonic phenomena, with qualitative agreement and fair quantitative accuracy as compared to the two-dimensional air flow.

RECOMMENDATIONS

(1) In view of the width of the bow and expansion waves, the chord of the model should be increased so that a smaller proportion of the pressure distribution is invalidated by these waves. A chord of at least 30 inches is recommended, though it is possible that in the transonic range a chord much greater than this would give trouble with waves reflected back to the model from the walls of the present channel.

(2) For rapid determination of the pressure distribution on an airfoil, where qualitative or rough quantitative results are desired, or for observation of phenomena occurring at particular stations along the airfoil, a photographic method, similar to one of those used, would be suitable. For most such purposes the use of even flood-lighting to illuminate the meniscus uniformly along its length, in conjunction with a camera shutter speed of one four-hundredth of a second, would give fair results. Sharper pictures could, however, be obtained by the use of two or more "Microflash" units (similar to that employed in the present work), or some other flash lighting system giving sufficient light, over a period of one thousandth of a second or less, to enable a camera aperture of at most $f8$ to be used.

(3) For more accurate quantitative data, a system of probes, placed at regular intervals along the model chord, should be used. Observations by this method are briefly described in Appendix II.

(4) Further tests at subsonic and low supersonic velocities

should be made before reliance is placed on tests made in the transonic region. For flows with detached shock, a method suggested by Ferri¹⁴ of evaluating the pressure drag from the shadow picture taken from above the model might be used.

14

Antonio Ferri, "Method for evaluating from Shadow or Schlieren Photographs the Pressure Drag in Two-dimensional or Axially Symmetrical Flow Phenomena with Detached Shock." NACA TM No. 1808, 1949

BIBLIOGRAPHY

A. Fundamental Theory

Ferri, Antonio, Elements of Aerodynamics of Supersonic Flows.
New York: The Macmillan Company, 1949. 434 pp.

Lamb, Horace, Hydrodynamics. Sixth Edition: London: Cambridge
University Press, 1932. 738 pp.

Liepmann, Hans Wolfgang, and Allen E. Puckett, Introduction to
Aerodynamics of a Compressible Fluid. New York: John Wiley
and Sons, Inc. 1947. 262 pp.

B. The Hydraulic Analogy

Binnie, A. M. and S. G. Hooker, "The Flow Under Gravity of an In-
compressible and Inviscid Fluid Through a Constriction in a
Horizontal Channel," Proceedings of the Royal Society, 159:
592-608, 1937.

Bruman, J. R. "Application of the Water Channel-Compressible Gas
Analogy". North American Aviation, Inc., Engineering Report,
No. NA-47-87, 1947. 60 pp.

Einstein, H. A. and E. H. Baird, "Progress Report of the Analogy
Between Surface Shock Waves on Liquids and Shocks in Compress-
ible Gases". California Institute of Technology Hydrodynamics
Laboratory Report. No. N-54, 1946. 68 pp.

Hatch, John Elmer, Jr., "The Application of the Hydraulic Analogies
to Problems of Two-Dimensional Compressible Gas Flow". Unpublished
Master's thesis, Georgia Institute of Technology, Atlanta, 1949.
57 pp.

Kantrowitz, Arthur, "The Formation and Stability of Normal Shock
Waves in Channel Flows". U.S. National Advisory Committee for
Aeronautics Technical Note No. 1225, 1947. 41 pp.

Orlin, W. James, Norman J. Linder and Jack G. Bitterly, "Applica-
tion of the Analogy Between Water Flow with a Free Surface and
Two-Dimensional Compressible Gas Flow". U.S. National Advisory
Committee for Aeronautics Technical Note No. 1185, 1947. 20 pp.

Preiswerk, Ernst "Application of the Methods of Gas Dynamics to Water Flows with Free Surface".

Part I. "Flows with No Energy Dissipation". U.S. National Advisory Committee for Aeronautics Technical Memorandum No. 934 1940. 69 pp.

Part II. "Flows with Momentum Discontinuities (Hydraulic Jumps)". U.S. National Advisory Committee for Aeronautics Technical Memorandum No. 935, 1940. 56 pp.

Riabouchinsky, D., "Mecanique des Fluides- Sur l'analogie hydraulique des mouvements d'un fluide compressible". Comptes Rendus, 195: 998-9. Paris, 1932.

Thomas, Gerald B., "Application of Water Channel-Compressible Gas Analogies to Problems of Supersonic Wind Tunnel Design". Unpublished Master's Thesis, Georgia Institute of Technology, Atlanta, 1949. 55 pp.

C. High Speed Wind Tunnel Test Results

Beavan, J. A. and G. A. M. Hyde, "Compressibility Increase of Lift and Moment on EC1250 for Low Speed 0.17". British Aeronautical Research Committee Reports and Memoranda No. 2055, 1942. 14 pp.

Beavan, J. A., G. A. M. Hyde and R. G. Fowler, "Pressure and Wake Measurements up to Mach Number 0.85 on an EC1250 Section with 25 per cent. Control". British Aeronautical Research Council Reports and Memoranda No. 2065, 1942. 46 pp.

Ferri, Antonio, "Investigations and Experiments in the Guidonia Supersonic Wind Tunnel". U.S. National Advisory Committee for Aeronautics Technical Memorandum No. 901, 1939. 19 pp.

———, "Experimental Results with Airfoils Tested in the High-Speed Tunnel at Guidonia". U.S. National Advisory Committee for Aeronautics Technical Memorandum No. 946, 1940. 14 pp.

———, "Completed Tabulation in the United States of Tests of 24 Airfoils at High Mach Numbers". U.S. National Advisory Committee for Aeronautics War-time Report No. L-143. 21 pp.

Graham, Donald J., Gerald E. Nitzberg and Robert N. Olson, "A Systematic Investigation of Pressure Distributions at High Speeds over Five Representative NACA Low-Drag and Conventional Airfoil Sections". U.S. National Advisory Committee for Aeronautics Technical Report No. 332, 1945. 68 pp.

- Hilton, W. F., "High-Speed Tunnel Balance Tests on N.A.C.A. 2218 Aerofoil". British Aeronautical Research Council Reports and Memoranda No. 1975, 1943. 4 pp.
- , "Subsonic and Supersonic Tests on $7\frac{1}{2}$ per cent. Biconvex Aerofoil". British Aeronautical Research Council Reports and Memoranda No. 2196, 1944. 8 pp.
- , "An Experimental Analysis of the Forces on Eighteen Aerofoils at High Speeds". British Aeronautical Research Council Reports and Memoranda No. 2058, 1946. 57 pp.
- , and F. W. Pruden, "Subsonic and Supersonic High Speed Tunnel Tests of a Faired Double Wedge Aerofoil". British Aeronautical Research Council Reports and Memoranda No. 2057, 1943. 13 pp.
- Knackstedt, W., "Examination and Evaluation of the Available Results with High-Velocity Flows". Headquarters Air Material Command Wright Field, Dayton, Ohio, Translation Report No. F-TS-1526-RE, 1947. 116 pp.
- Liepmann, H. W., H. Askenas and J. D. Cole, "Experiments in Transonic Flow". United States Air Force Air Material Command Wright-Patterson Air Force Base, Dayton, Ohio, Technical Report No. 5667, 126 pp.
- Lindsey, W. F., Bernard N. Daley and Milton D. Humphreys, "The Flow and Force Characteristics of Supersonic Airfoils at High Subsonic Speeds". U.S. National Advisory Committee for Aeronautics Technical Note No. 1211, 1947. 15 pp.
- Lindsey, W. F., D. B. Stevenson, and Bernard N. Daley, "Aerodynamic Characteristics of 24 N.A.C.A. 16-Series Airfoils at Mach Numbers Between 0.3 and 0.8". U.S. National Advisory Committee for Aeronautics Technical Note No. 1546, 1948. 86 pp.
- Pearcey, H. H., "Drag Measurements on N.A.C.A. 2218 Section at Compressibility Speeds for Comparison with Flight Tests and Theory". British Aeronautical Research Council Reports and Memoranda No. 2093, 1943. 9 pp.
- Stack, John and W. F. Lindsey, "Tests of N-85, N-86, and N-87 Airfoil Sections in the 11-inch High Speed Wind Tunnel". U.S. National Advisory Committee for Aeronautics Technical Note No. 665, 1938. 6 pp.
- Stack, John and Albert E. von Doenhoff, "Tests of 16 Related Aerofoils at High Speeds". U.S. National Advisory Committee for Aeronautics Technical Report No. 492, 1934. 23 pp.

Thompson, J. S., M. Markowicz, J. A. Beavan and R. G. Fowler, "Pressure Distribution and Wake Traverses on Models of Mustang Wing Section in the Royal Aircraft Establishment and National Physical Laboratory High Speed Tunnels". British Aeronautical Research Council Reports and Memoranda No. 2251, 1944. 47 pp.

D. Other References

Bonney, E. Arthur, "Aerodynamic Characteristics of Rectangular Wings at Supersonic Speeds", Journal of the Aeronautical Sciences, 14: 110-16, 1947.

Ferri, Antonio, "Method for Evaluating from Shadow or Schlieren Photographs the Pressure Drag in Two-Dimensional or Axially Symmetrical Flow Phenomena with Detached Shock". U.S. National Advisory Committee for Aeronautics Technical Note No. 1808, 1949. 14 pp.

APPENDIX I

TABLES

TABLE I

SAMPLE CALCULATION OF PRESSURE COEFFICIENTS

FROM EXPERIMENTAL DATA

G.U.3 Airfoil, Upper surface, $\alpha = -2^\circ$

$$d_s = 0.239 \text{ ins.}$$

$$\text{Timer reading} = 1.98 \text{ secs.}$$

$$\text{Timer cam length} = 2.94 \text{ ft.}$$

$$\therefore M_s = \frac{\frac{2.94}{1.98}}{\sqrt{g \times \frac{0.239}{12}}} = 1.85$$

$$\frac{1}{M_s^2} = 0.2922$$

$$C_p = \frac{1}{M_s^2} \left[\left(\frac{d_t}{d_s} \right)^2 - 1 \right] \quad [Eqn. (9)]$$

Station (% chord)	d_t (ins)	$\frac{d_t}{d_s}$	$\left(\frac{d_t}{d_s} \right)^2 - 1$	C_p
0	0.415	1.736	2.014	0.588
0.1	0.461	1.929	2.721	0.795
0.2	0.384	1.607	1.582	0.462
0.3	0.297	1.243	0.545	0.159
0.4	0.284	1.188	0.411	0.120
0.5	0.261	1.092	0.1925	0.056
0.6	0.261	1.092	0.1925	0.056
0.7	0.252	1.054	0.1109	0.032
0.8	0.239	1.000	-0-	-0-
0.9	0.231	0.967	-0.649	-0.019
1.0	0.229	0.953	-0.0822	-0.024

TABLE II

EXPERIMENTAL VALUES OF LIFT, DRAG AND MOMENT

COEFFICIENTS FOR G.U.3 AIRFOIL

 $M = 1.85$

α (Degrees)	C_L	C_D	C_m
-2	-0.162	0.054	0.019
0	-0.111	0.050	-0.009
2	0.042	0.035	-0.021
6	0.038	0.046	-0.084
10	0.252	0.072	-0.143
16	0.549	0.185	-0.297

 $M = 2.13$

α (Degrees)	C_L	C_D	C_m
-2	-0.153	0.050	0.018
0	-0.138	0.042	0.018
2	-0.074	0.033	-0.010
6	0.072	0.030	-0.064
10	0.253	0.065	-0.144
16	0.440	0.147	-0.252

TABLE III

EXPERIMENTAL VALUES OF LIFT, DRAG AND MOMENT

COEFFICIENTS FOR G.U.4 AIRFOIL

 $M = 1.85$

α (Degrees)	C_L	C_D	C_m
0	-0.034	0.0167	-0.017
2	0.042	0.0205	-0.041
10	0.347	0.0735	-0.147

 $M = 2.13$

α (Degrees)	C_L	C_D	C_m
0	-0.044	0.0135	-0.010
2	0.067	0.0131	-0.045
10	0.278	0.0513	-0.120

APPENDIX II

BRIEF DESCRIPTION OF FURTHER EXPERIMENTS

USING PROBES FOR DETERMINATION OF LOCAL WATER DEPTH

BRIEF DESCRIPTION OF FURTHER EXPERIMENTS
USING PROBES FOR DETERMINATION OF LOCAL WATER DEPTH

Objective

In view of the necessity for greater accuracy in measuring the local depth about the model, and in particular for avoiding if possible the effect of the meniscus, it was decided to use a different method of measurement. In addition, some stiffening of the model support seemed desirable, to reduce angle of attack errors.

Equipment

Steel needle probes were attached to a brass plate by means of adjustable brass screws, and this plate was screwed to the top of the model. The probes were so placed as to be at 0.1 chord intervals, and 0.1 inch from the airfoil surface. The arrangement is shown in Figure 17.

The model support was stiffened, and provision was made for screw adjustment of the angle of attack. A board, enabling a prone position of the operator above the test section, was fixed to the original observation platform, and the motor controls were moved so as to be convenient for this position.

The remaining equipment was as previously described, except that no photographic equipment was required.

Procedure

The model was set up and run as before, but several runs were

at each condition (i.e. of angle of attack and Mach number), and during the runs the probes were adjusted so that, at the test section, each of them was just touching the water, as shown by the small disturbance it caused.

Discussion.

The pressure plots obtained by the probe method for the G.U.3 airfoil at $M = 2.13$ and $\alpha = -2, 0$, and $+6$ degrees, are presented in Figures 18, 19, and 20 respectively, with comparison curves from Ferri's wind tunnel results. The plots for the G.U.4 airfoil at $M = 1.85$ and $\alpha = -2, 0$ and $+6$ degrees are presented in Figures 21, 22, and 23, with comparison theoretical curves (no wind tunnel pressure plots being available for this airfoil).

While some scatter of the point remains, it is seen that the results obtained with this method agree considerably more closely with the theoretical and wind tunnel results than do the results from the photographic technique described in the main body of this thesis. The meniscus connection having been avoided by the use of probes, the scatter of the points is about the expected mean line, except in regions of sharp flow turn.

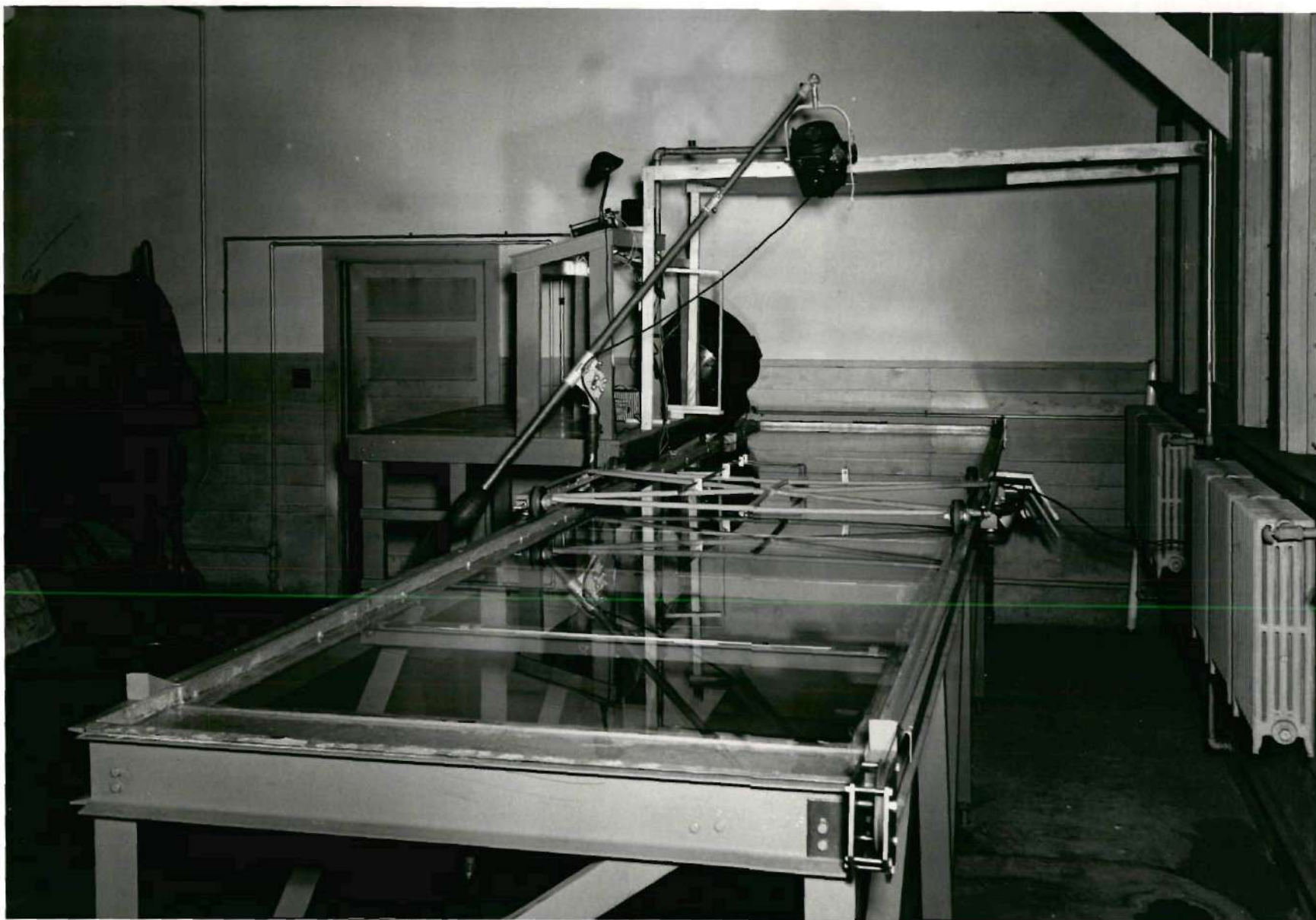
Thus the lift, drag and moment coefficients must necessarily agree more closely than previously with the theoretical or wind tunnel results and agreement with the latter is more likely in view of the closer agreement of the water channel and wind tunnel results at the trailing edge.

The probe method thus represents a considerable improvement upon the photographic method of local depth measurement, and its use

is recommended where accurate quantitative results are desired.

APPENDIX III

FIGURES



40

FIGURE 1
GENERAL VIEW OF WATER CHANNEL

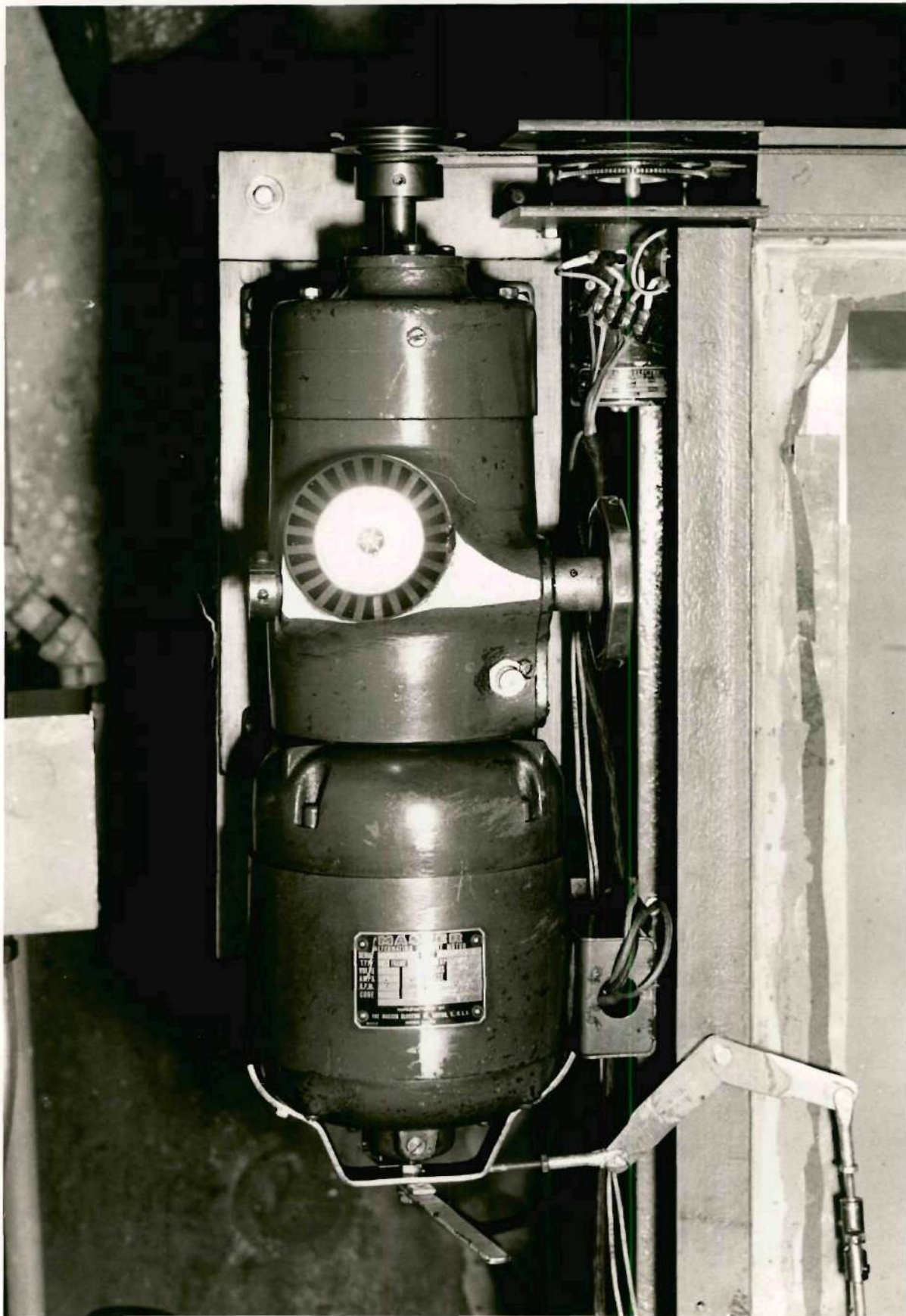


FIGURE 2

CARRIAGE DRIVE MECHANISM

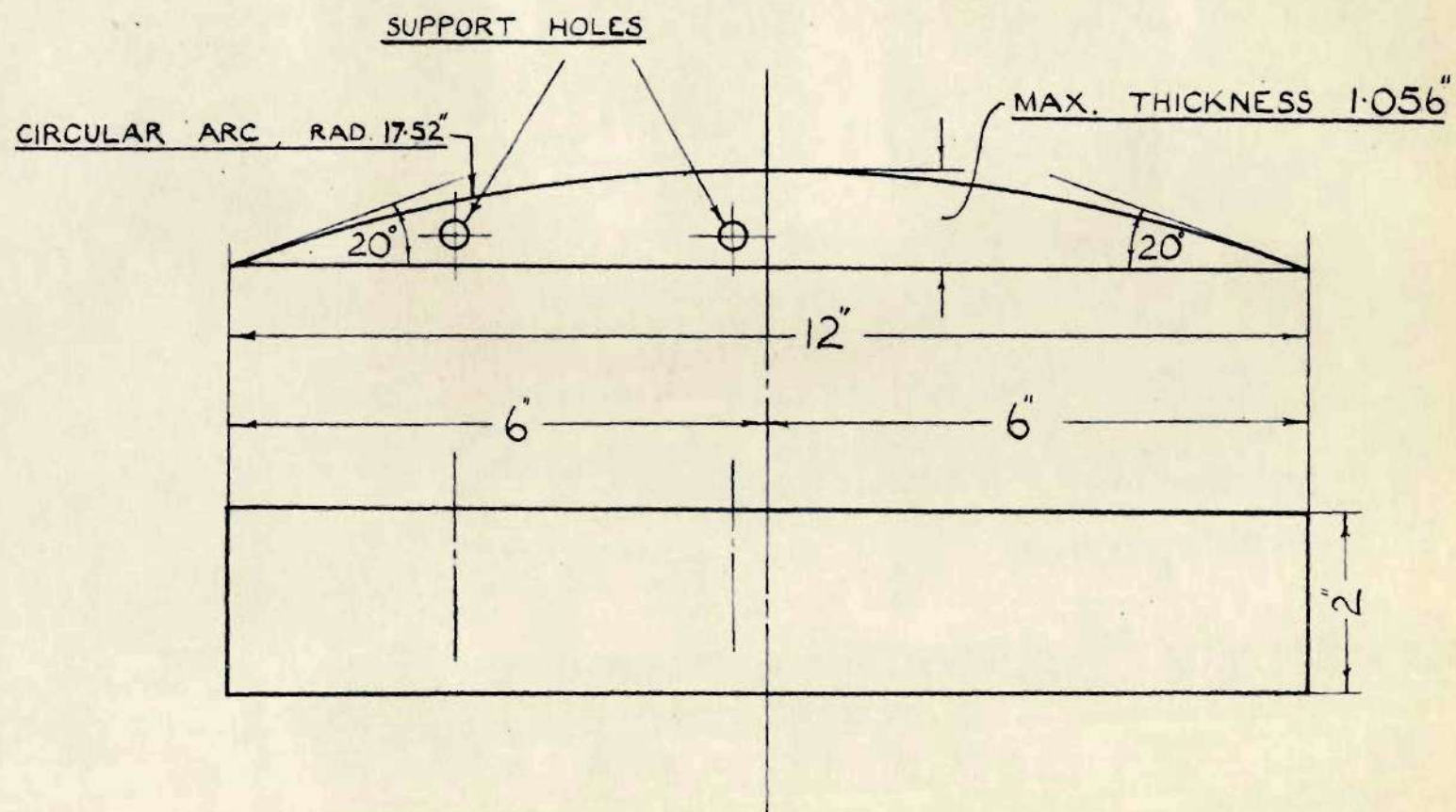


FIGURE 3. G.U.3 AIRFOIL MODEL

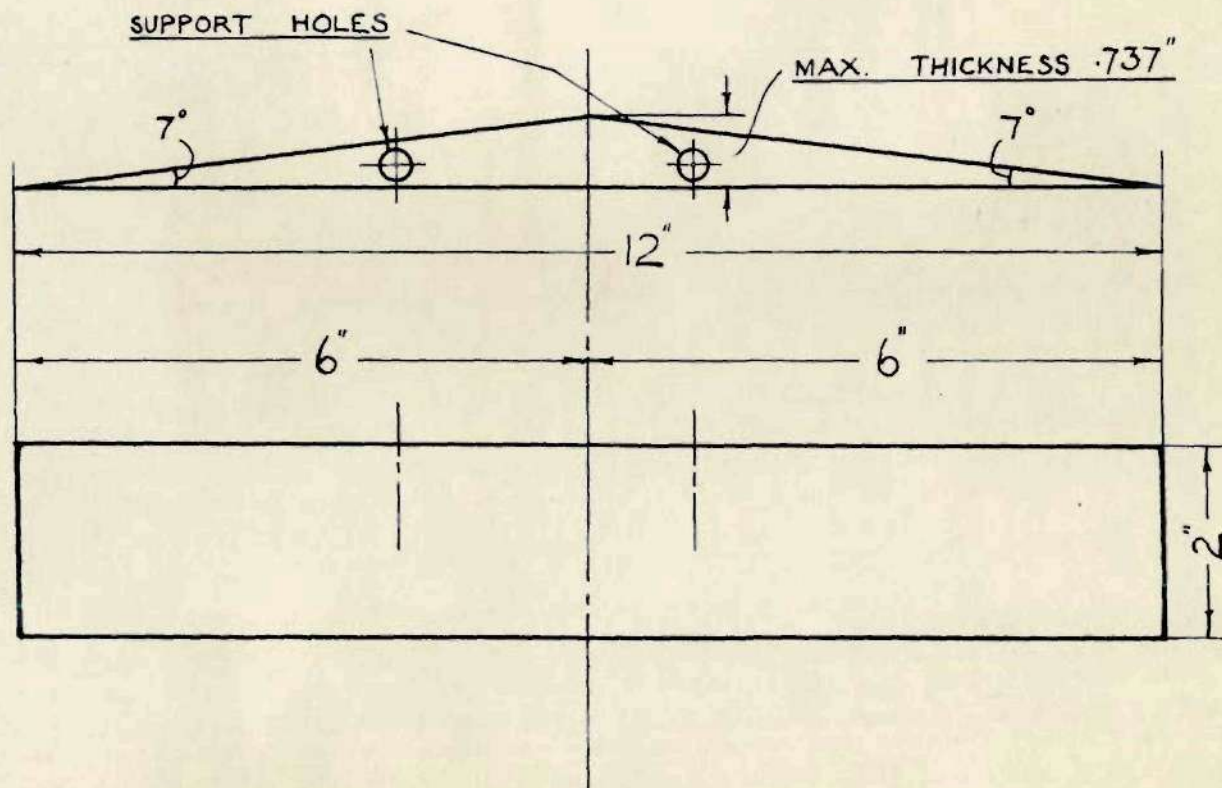
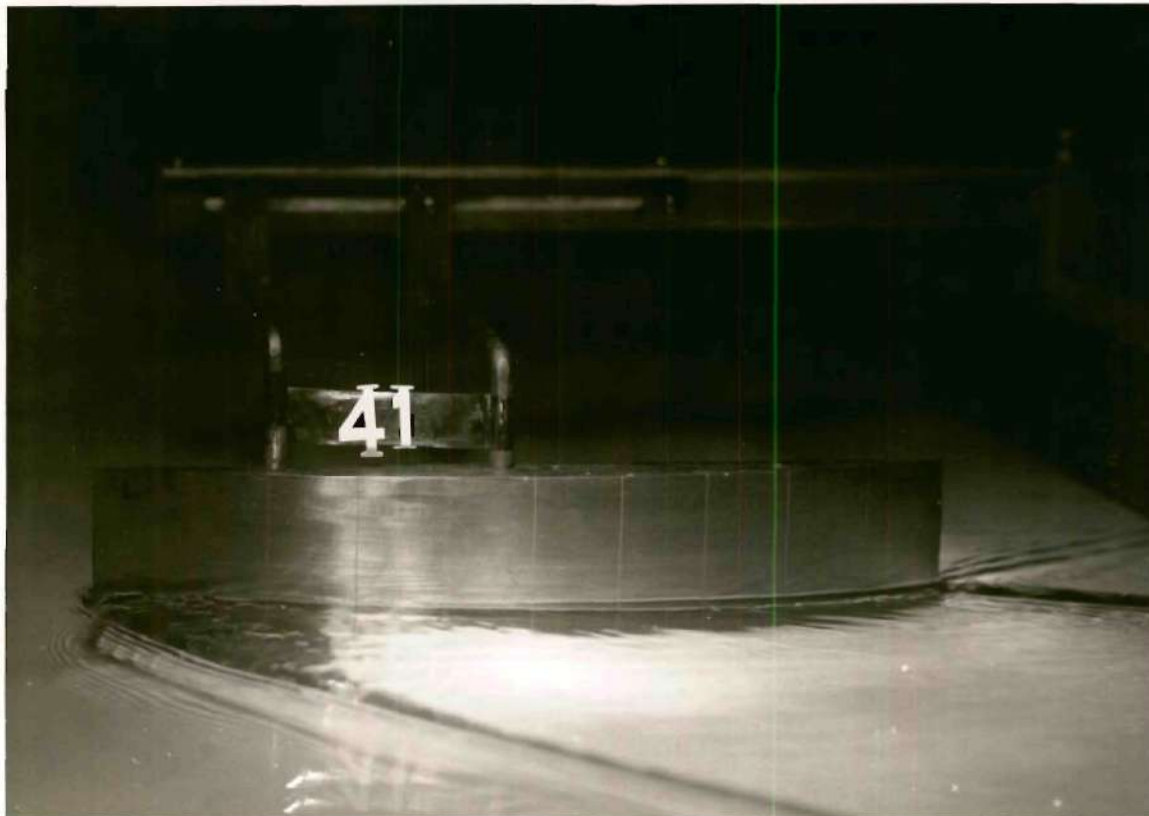
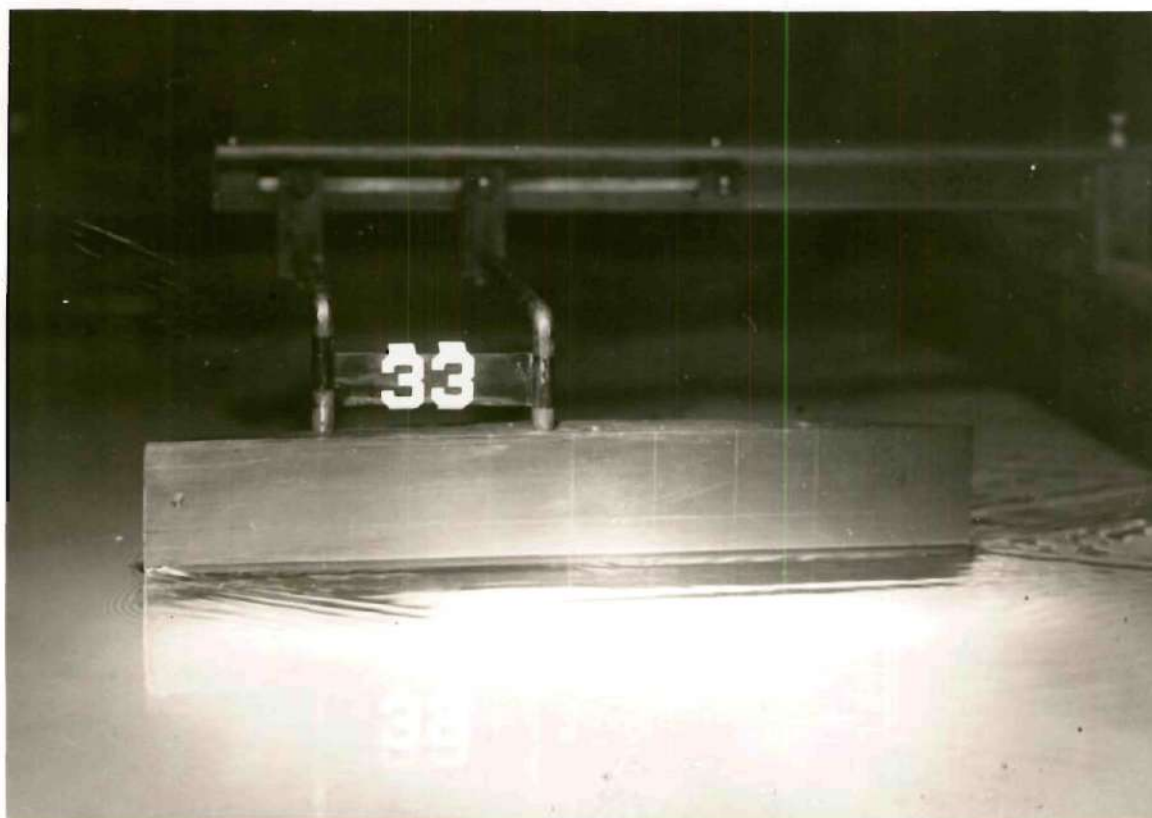


FIGURE 4. G.U.4 AIRFOIL MODEL

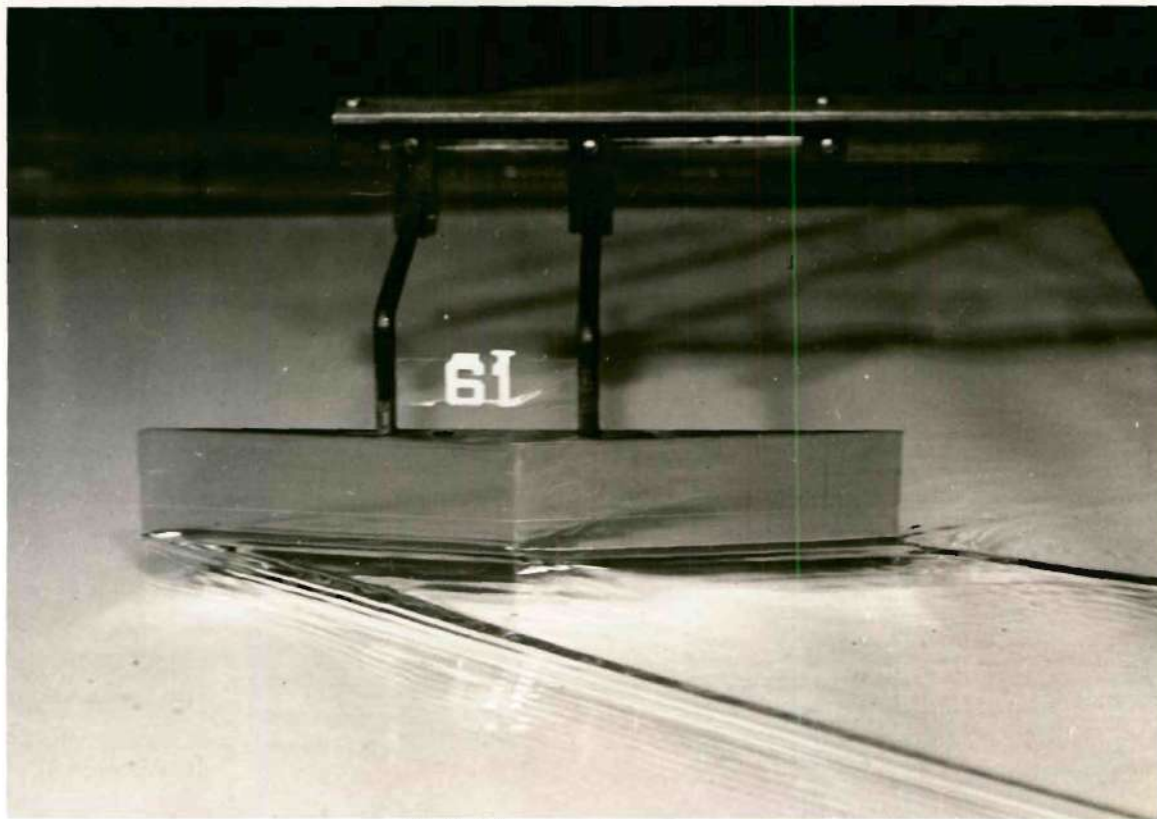


(a) Upper Surface

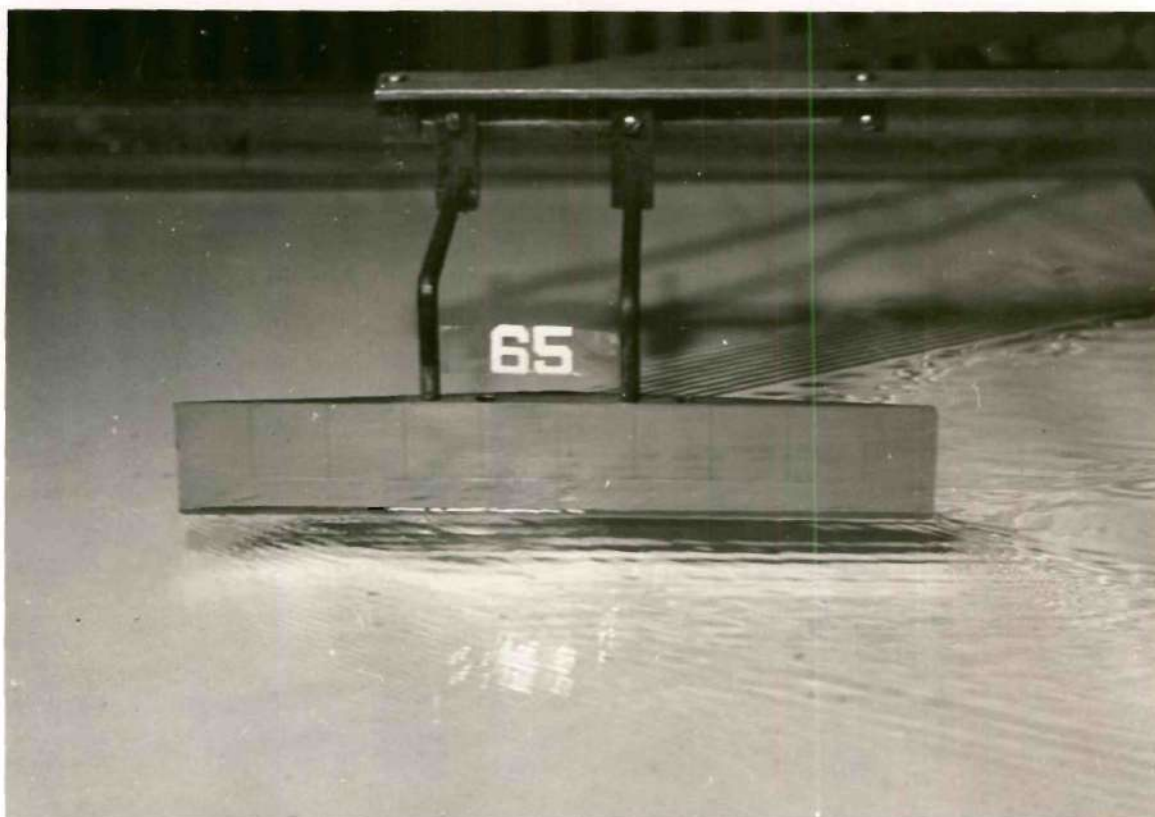


(b) Lower Surface

FIGURE 5
FLOW ABOUT G.U.3 AIRFOIL AT M 1.85, -2



(a) Upper Surface



(b) Lower Surface

FIGURE 6
FLOW ABOUT G.U.4 AIRFOIL AT M 2.13, 0

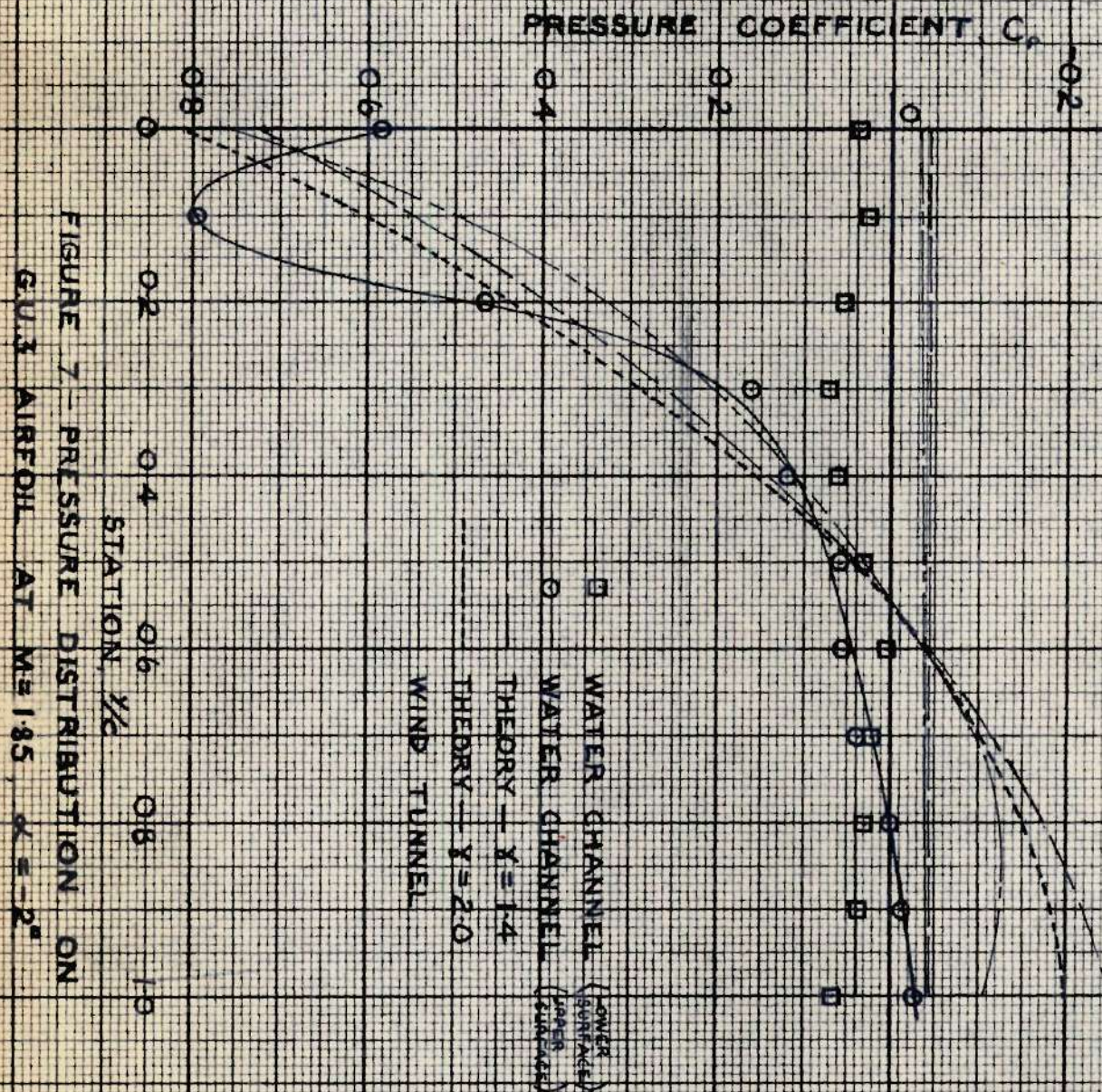


FIGURE 7 - PRESSURE DISTRIBUTION ON
 G.U.3 AIRFOIL AT $M=1.85$, $\alpha=-2^\circ$

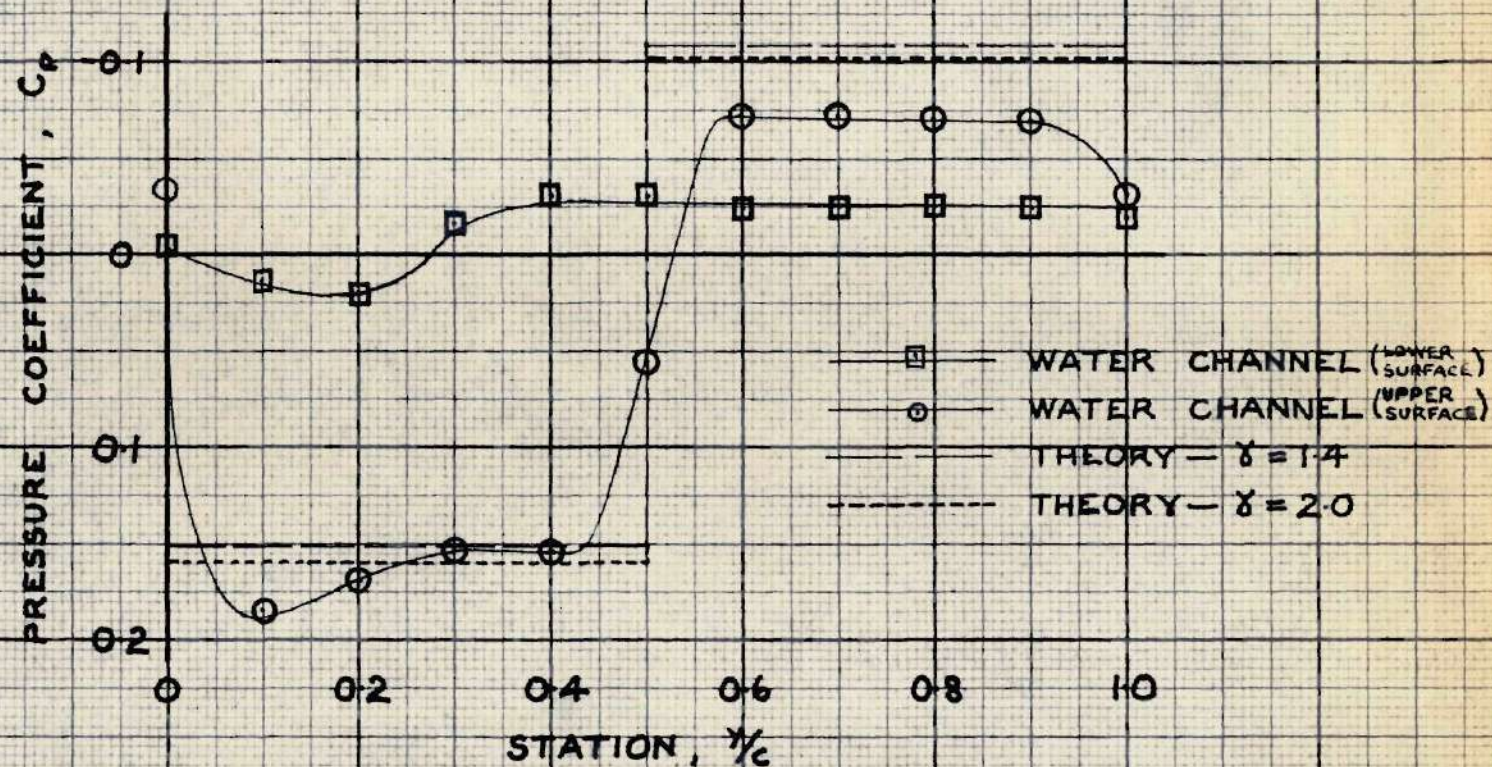


FIGURE 8—PRESSURE DISTRIBUTION ON
G.U.4 AIRFOIL AT $M = 2.13$, $\alpha = 0^\circ$

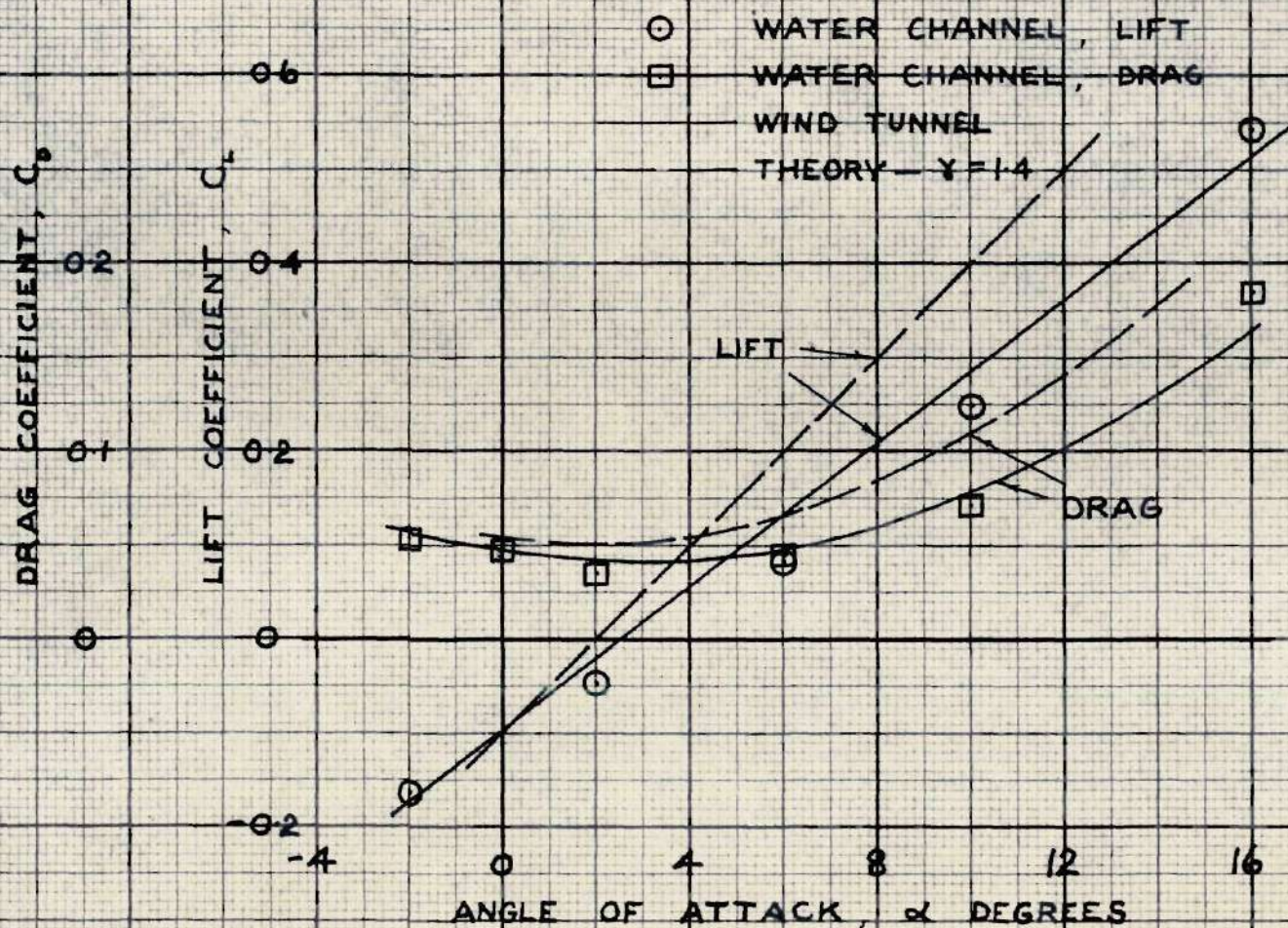


FIGURE 9.— LIFT AND DRAG CURVES FOR
G.U.3 AIRFOIL AT $M = 1.85$

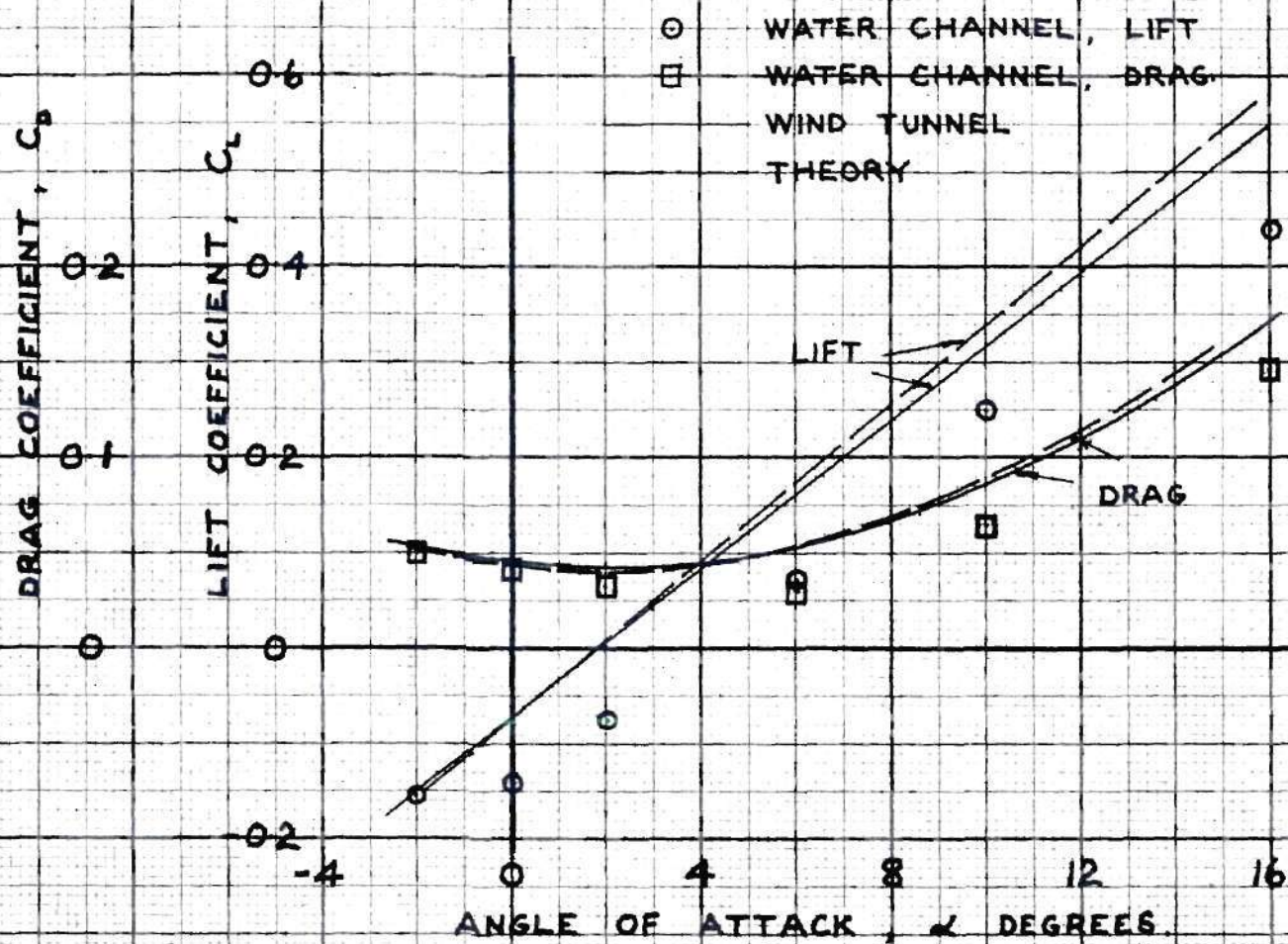


FIGURE 10. LIFT AND DRAG CURVES FOR
G.U.3. AIRFOIL AT $M = 2.13$

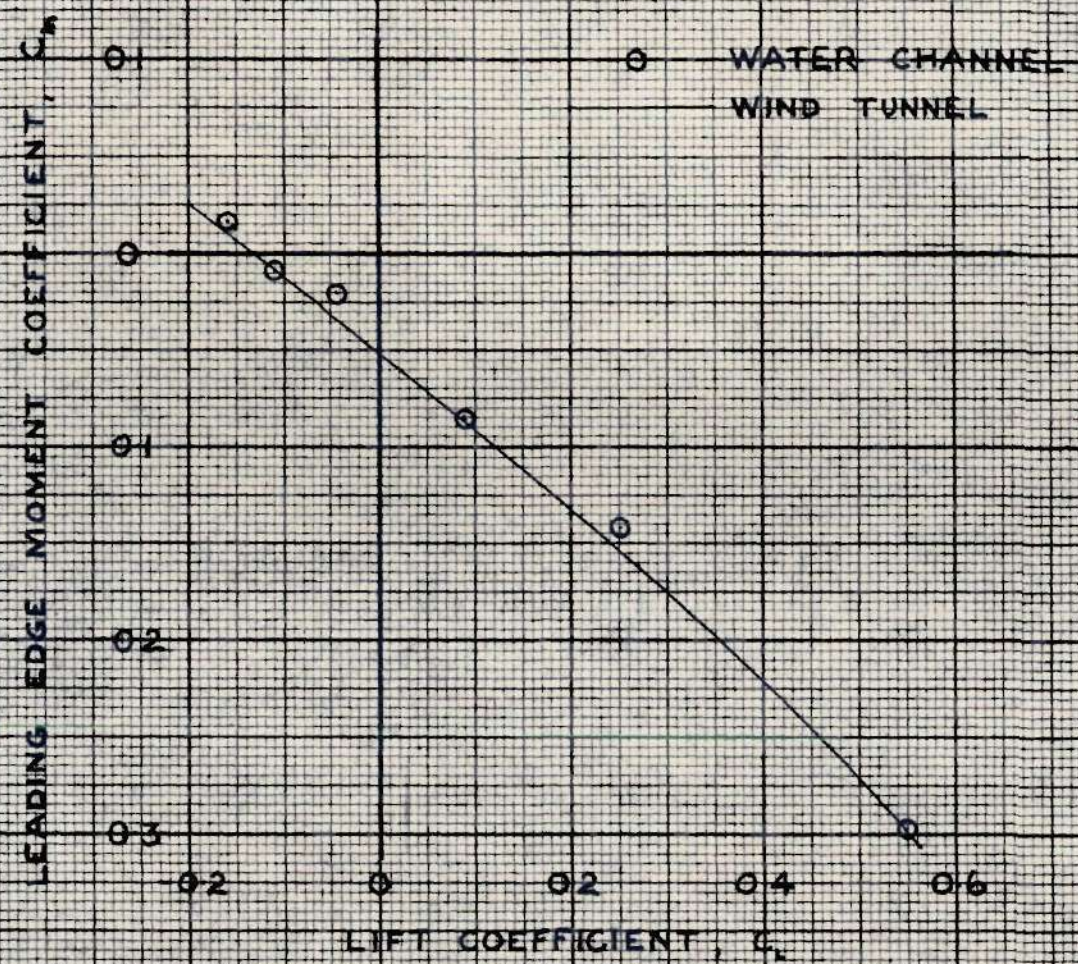


FIGURE 11. MOMENT CURVES FOR
G.U.3 AIRFOIL AT $M=1.85$

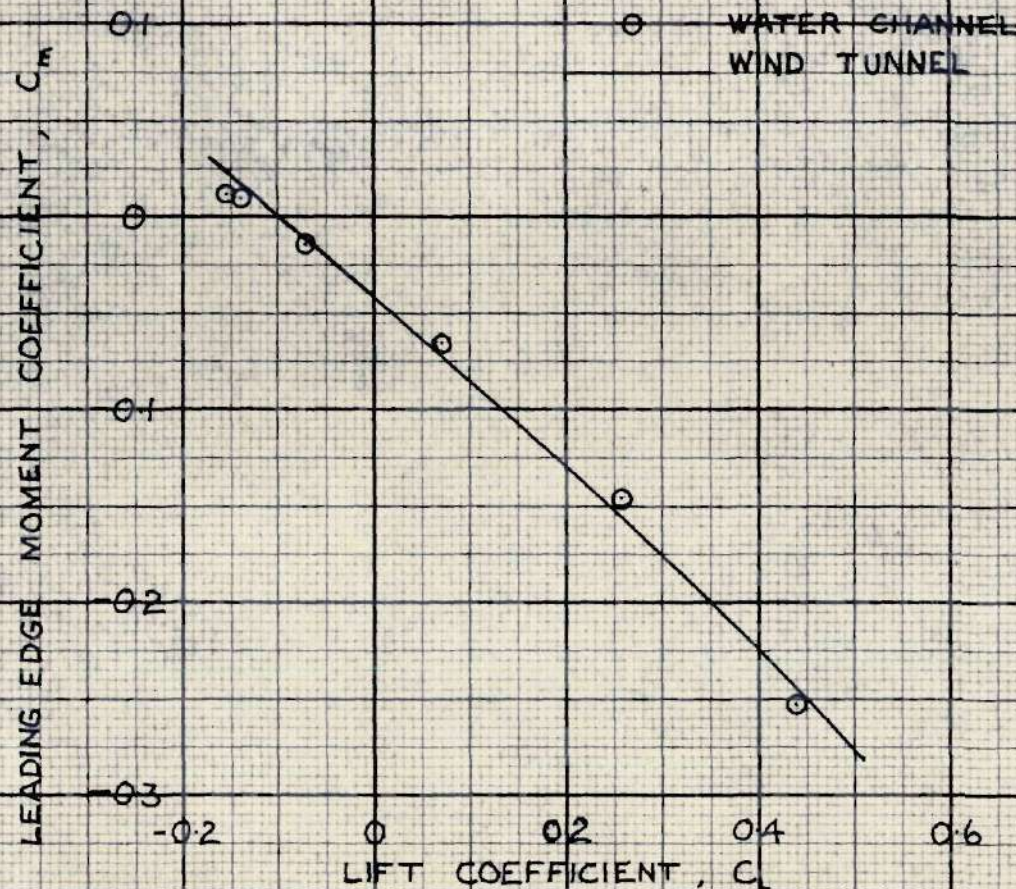


FIGURE 12.—MOMENT CURVES FOR
G.U.3 AIRFOIL AT $M=2.3$

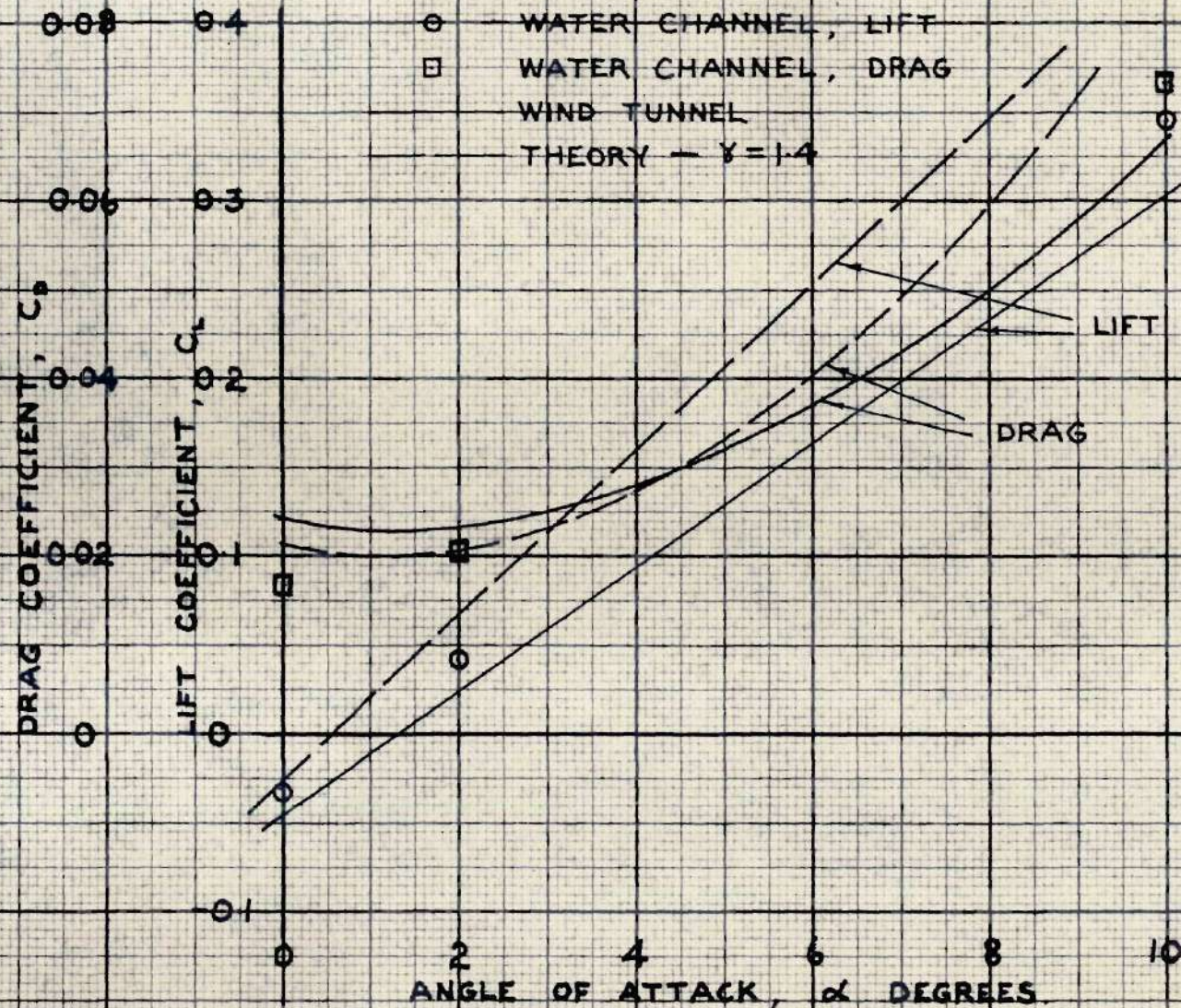


FIGURE 13.—LIFT AND DRAG CURVES FOR
 G.U.4 AIRFOIL AT $M=1.85$

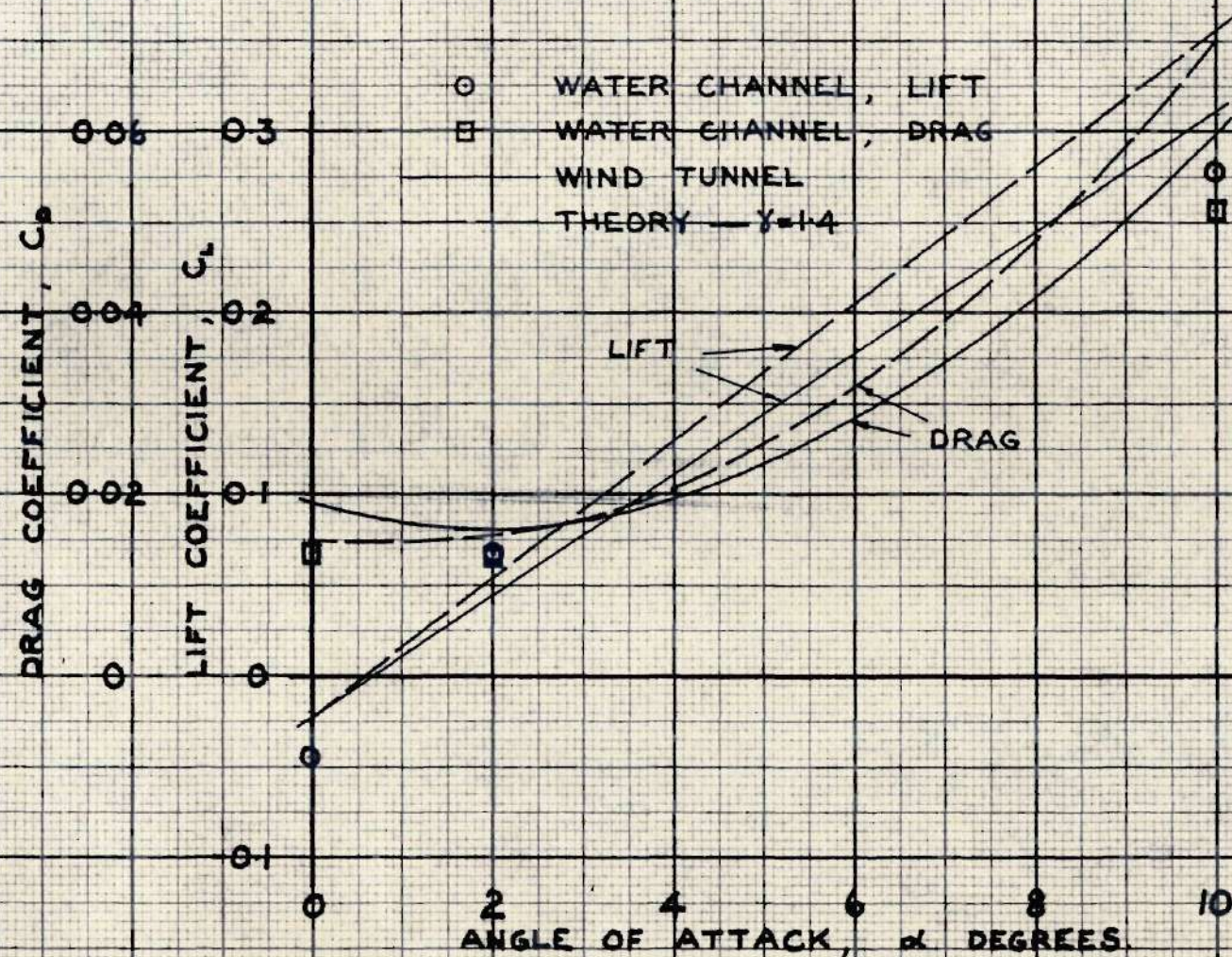


FIGURE 14—LIFT AND DRAG CURVES FOR
G.U.4 AIRFOIL AT $M=2.13$

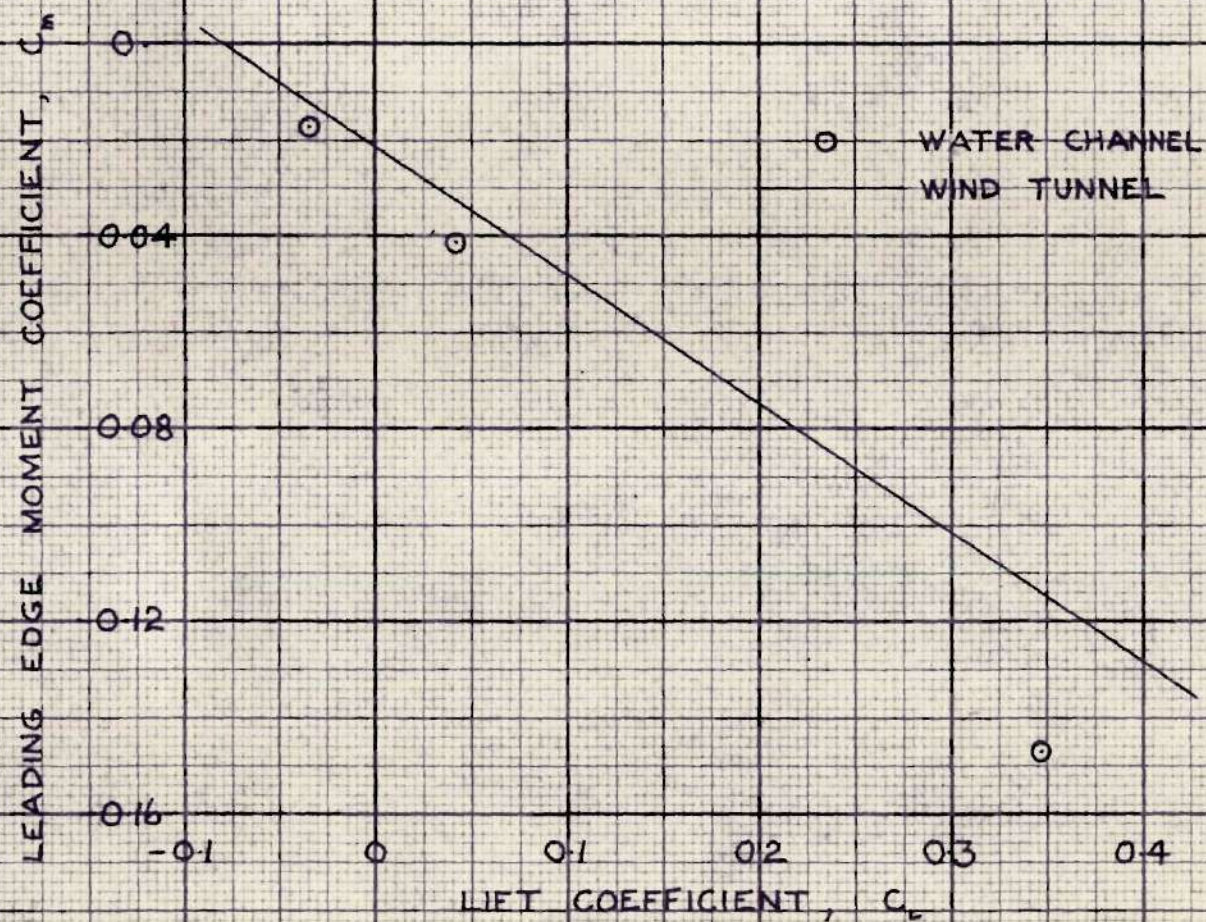


FIGURE 15.—MOMENT CURVES FOR
G.U.4 AIRFOIL AT $M=1.85$

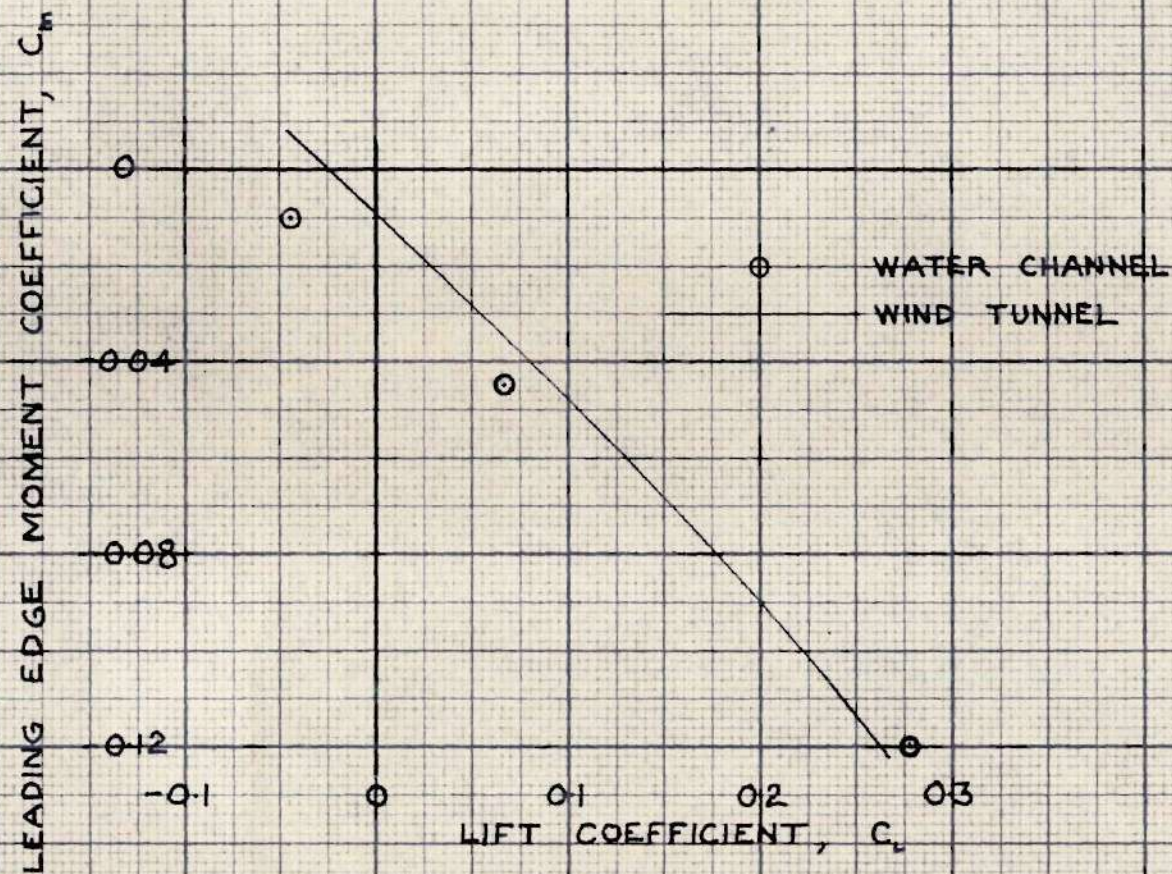


FIGURE 16.- MOMENT CURVES FOR
G.U.4 AIRFOIL AT $M = 2.13$



FIGURE 17

VIEW OF MODEL WITH PROBES IN POSITION

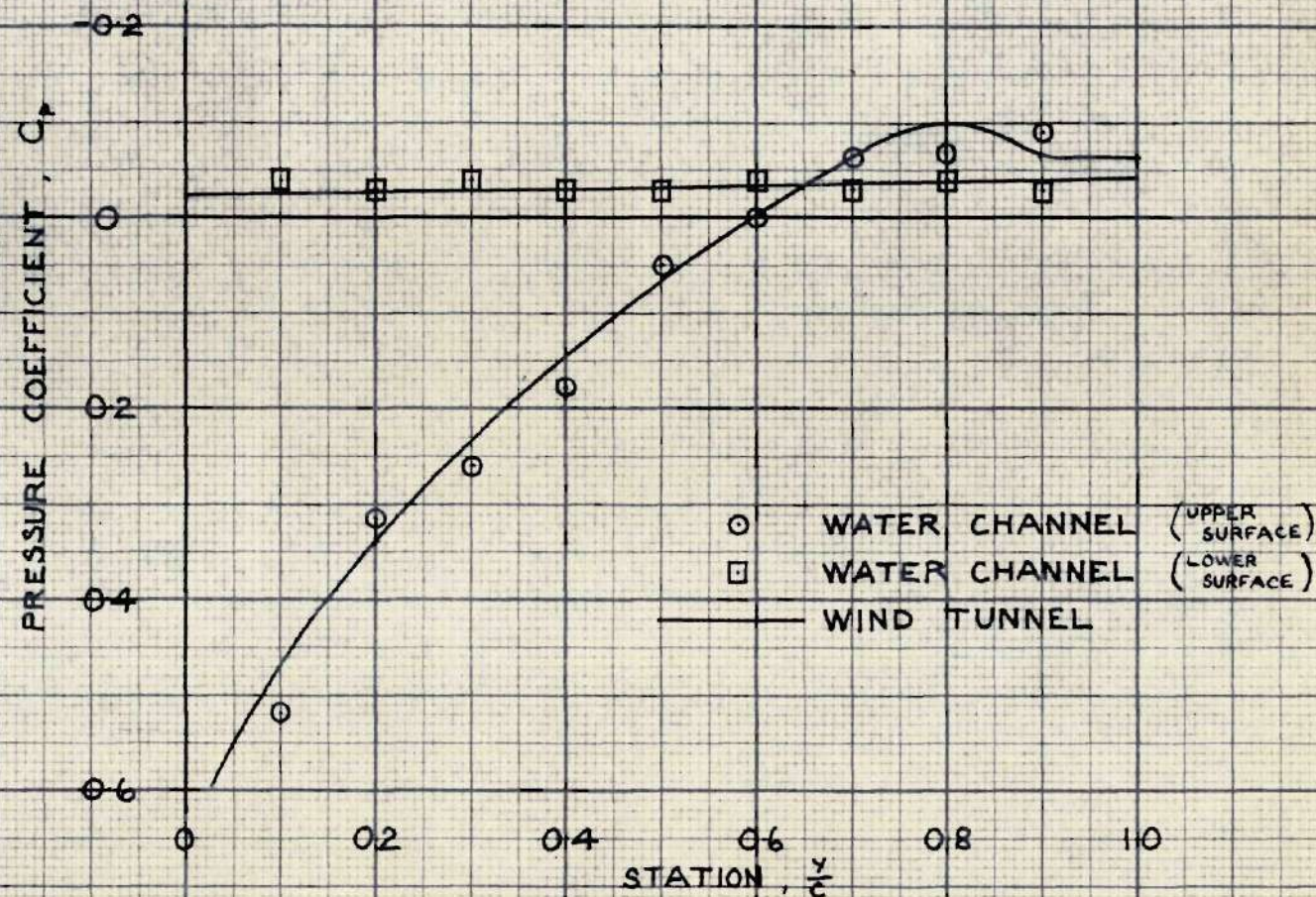


FIGURE 18.—PRESSURE DISTRIBUTION ON
G.U.3 AIRFOIL AT $M=2.13$, $\alpha=-2^\circ$: PROBE METHOD

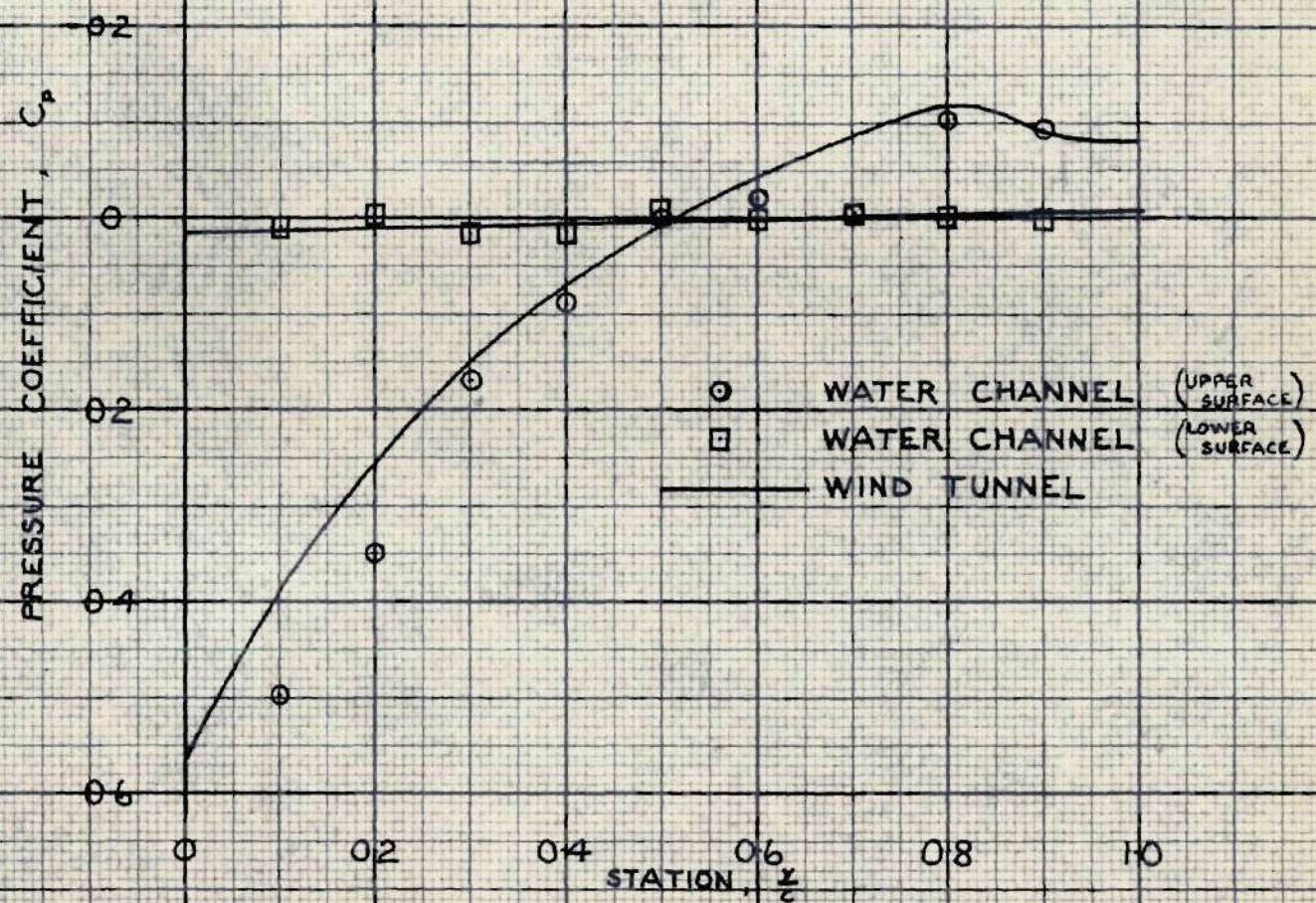


FIGURE 19.— PRESSURE DISTRIBUTION ON
G.03 AIRFOIL AT $M = 2.13$, $\alpha = 0^\circ$: PROBE METHOD

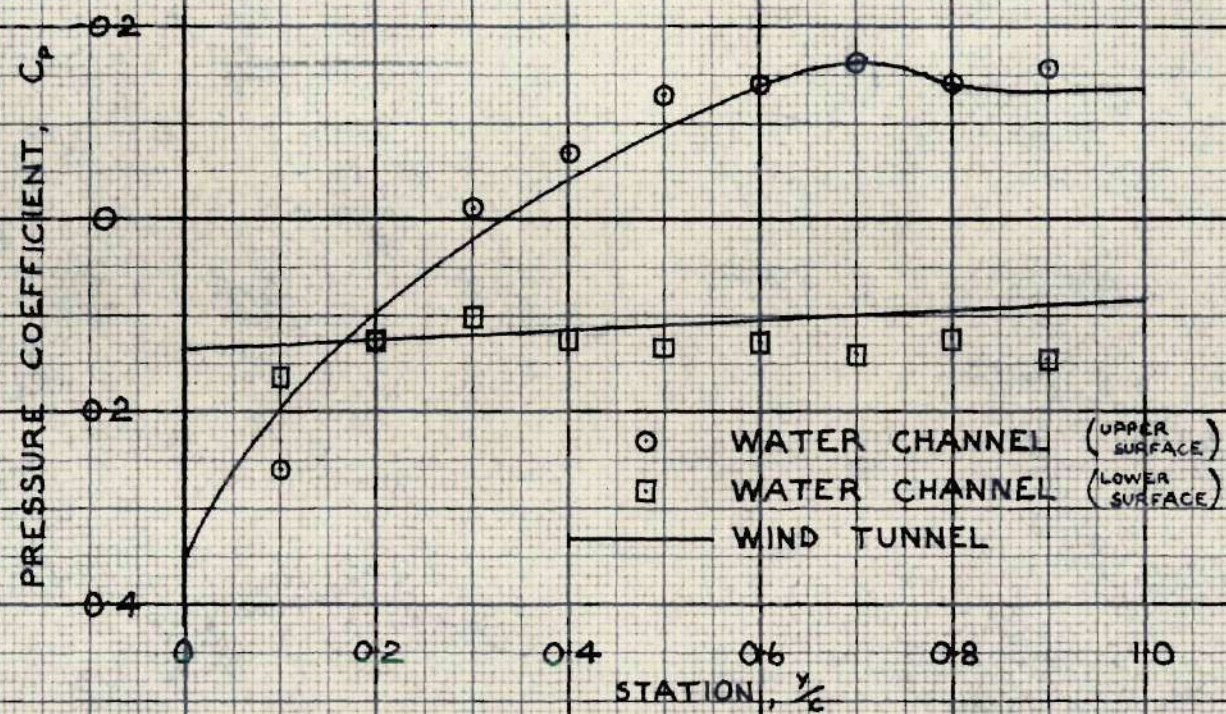


FIGURE 20.—PRESSURE DISTRIBUTION ON
G.U.3 AIRFOIL AT $M=2.13$, $\alpha = +6^\circ$: PROBE METHOD.

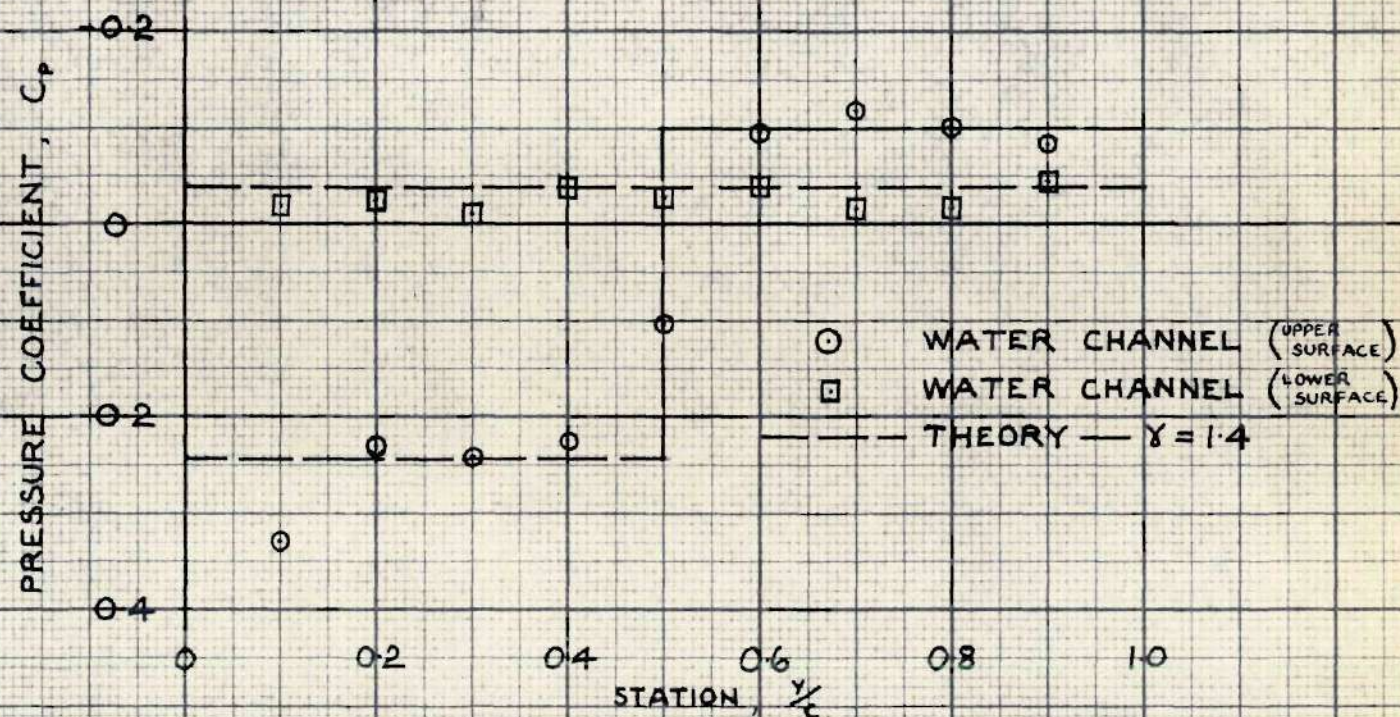


FIGURE 21.— PRESSURE DISTRIBUTION ON
 G.U.4 AIRFOIL AT $M = 1.85$, $\alpha = -2^\circ$: PROBE METHOD.

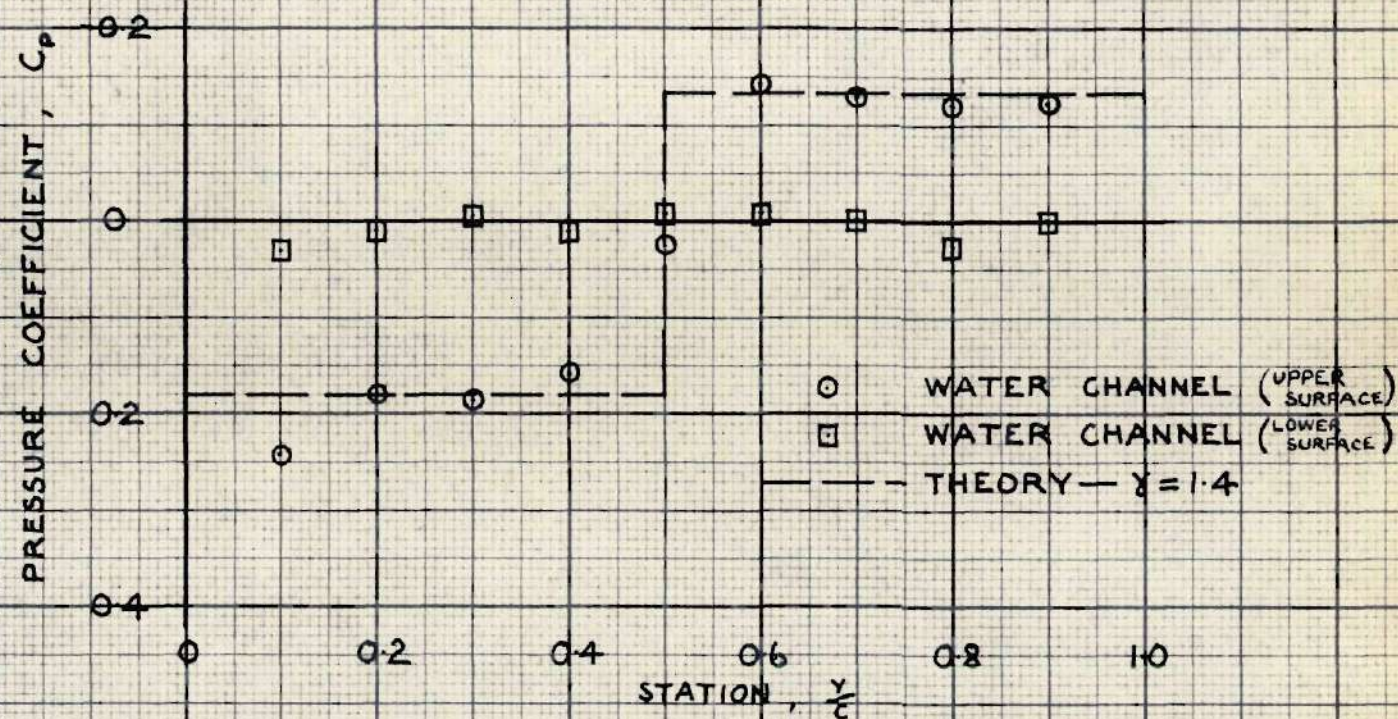


FIGURE 22.—PRESSURE DISTRIBUTION ON
 G.U.4 AIRFOIL AT $M = 1.85$, $\alpha = 0^\circ$: PROBE METHOD

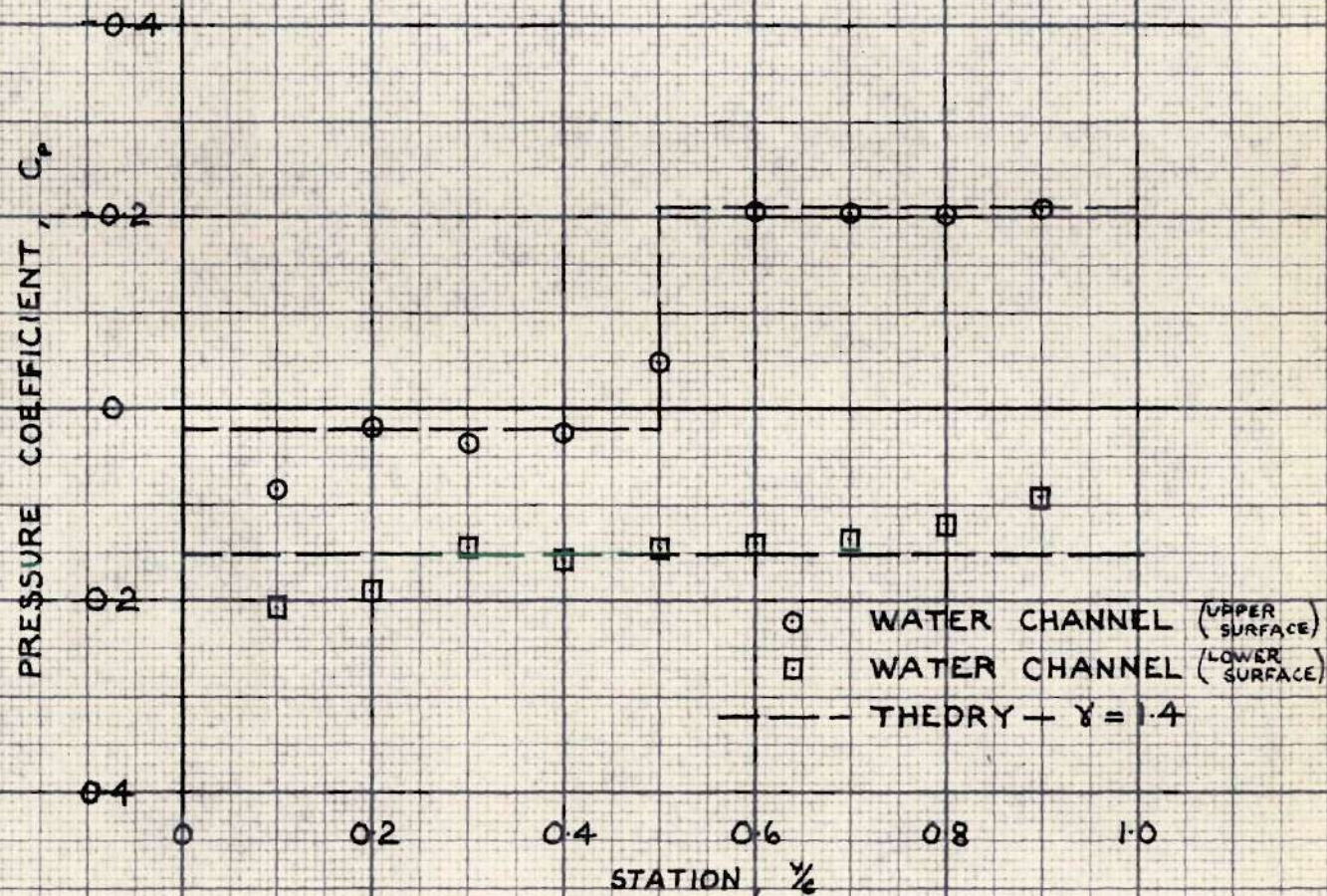


FIGURE 23.—PRESSURE DISTRIBUTION ON
G.U.4 AIRFOIL AT $M=1.85$, $\alpha = +6^\circ$: PROBE METHOD